

ABSTRACT

Title of Thesis: DEVELOPING TOOLS FOR INVESTIGATING CHEMOTAXIS
SIGNAL CLUSTERS IN *BACILLUS SUBTILIS*

James A. Rogers, Jr., Master of Science, 2012

Thesis directed by: Associate Professor Richard C. Stewart
Department of Cell Biology and Molecular Genetics

Many bacteria make use of a set of dedicated chemoreceptor proteins to control a His-Asp signaling system; this control converts environmental sensory information into instructions that regulate flagellar rotation, enabling chemotaxis. This thesis summarizes my investigations of some of the chemotaxis signaling proteins in *Bacillus subtilis*, particularly coupling proteins CheW and CheV. Proteins CheA, CheW, CheV, CheY, and FliM were each expressed in *B. subtilis* as translational fusions with either YFP or CFP. These fusion proteins were then shown to fluoresce in living bacterial cells. Motility experiments were conducted to compare the function of these fusion proteins to their wild type counterparts. This thesis proposes a series of experiments that would use these fluorescent fusion proteins to further explore the idea that these chemotaxis proteins change position when *B. subtilis* encounters chemostimuli.

DEVELOPING TOOLS FOR INVESTIGATING CHEMOTAXIS SIGNAL CLUSTERS
IN *BACILLUS SUBTILIS*

by

James A. Rogers, Jr.

Thesis submitted to the Faculty of the Graduate School of the
University of Maryland, College Park in partial fulfillment
of the requirements for the degree of
Master of Science
2012

Advisory Committee:

Associate Professor Richard C. Stewart, Chair
Associate Professor Kevin S. McIver
Professor Stephen Wolniak

©Copyright by

James A. Rogers, Jr.

2012

Acknowledgements

First and foremost, I would like to thank my family and friends for supporting me throughout all my years in graduate school. My parents deserve special recognition for encouraging me endlessly, yet allowing me to find my own path.

I would also like to thank my advisor, Dr. Stewart, for taking me on and helping me develop my research plan. I learned an enormous amount about academic research in his laboratory.

Thanks to my lab mates in the Stewart lab. Nicole, Ian, Petya, Anna, Saunam, and Camille, both your company and your hard work made long hours in the lab run quicker.

Lastly, thanks to all the members of my research committee. Your comments, questions, and suggestions often pointed me down new research paths I would have never considered without your guidance.

Table of Contents

Acknowledgements	ii
Table of Contents	iii
List of Figures	v
List of Tables	vi
Chapter 1: Introduction	1
How Do Bacteria Navigate Their Environment?.....	1
The Mechanics of Chemotaxis Signaling.....	1
Why Do We Study <i>B. subtilis</i> Chemotaxis?	3
The Genomic Organization of <i>B. subtilis</i> Chemotaxis Genes.....	5
The Current Model for <i>B. subtilis</i> Chemotaxis Signaling.....	6
What Are the Mechanisms of Signal Adaptation in <i>B. subtilis</i> ?.....	9
Comparing Methods for Labeling Intracellular Proteins.....	12
Chapter 2: Experimental Methods	16
PCR Cloning and Bacterial Transformation.....	16
Site-Directed Mutagenesis.....	19
Motility Agar Assays.....	20
Fluorescence Microscopy.....	21
Chapter 3: Results and Discussion	22
Developing a <i>cheA</i> Deletion Strain.....	22
Design and Characterization of <i>cheA</i> Translational Fusions.....	23
Developing a <i>cheW</i> Deletion Strain.....	26
Design and Characterization of <i>cheW</i> Translational Fusions.....	27
Developing a <i>cheV</i> Deletion Strain.....	29
Design and Characterization of <i>cheV</i> Translational Fusions.....	30
Developing a <i>cheY</i> Deletion Strain.....	32
Design and Characterization of <i>cheY</i> Translational Fusions.....	33
Developing a <i>fliM</i> Deletion Strain.....	35
Design and Characterization of <i>fliM</i> Translational Fusions.....	36
Fluorescence Microscopy.....	38
Discussion of Results.....	41

Chapter 4: Future Directions	43
Objective 1: Identify the Clustering Behavior of <i>B. subtilis</i> Coupling Proteins Throughout the Cycle of Stimulation and Adaptation.....	43
Strain Design and Qualification.....	44
Objective 2: Develop a FRET Assay to Monitor <i>B. subtilis</i> Chemostimulus Response and Adaptation.....	49
In Regard to Results from Chapter 3.....	49
Constructing a FRET Assay to Monitor the Interaction Between CheY and FlmM <i>in vivo</i>	50
Identifying the Contributions of Several Adaptation Mechanism in <i>B. subtilis</i> Chemotaxis.....	53
Summary.....	54
Appendix A (Table 3: List of Primers Used in this Work)	56
Appendix B (Contributors to this Work)	59
Bibliography	60

List of Figures

- Figure 1 A cartoon of the primary components in the *B. subtilis* chemotaxis circuit.
- Figure 2 Organization of the *fla/che* operon.
- Figure 3 A more detailed model of the *B. subtilis* chemotaxis signaling circuit.
- Figure 4 Step-wise model for stimulation and adaptation.
- Figure 5 A cartoon diagram of *cheV* in *B. subtilis*.
- Figure 6 Plasmid map of pHCMC04.
- Figure 7 Template for Xer-cise deletion construct.
- Figure 8 Complementation of $\Delta cheA$ by CheA and CheA- fluorescent fusions.
- Figure 9 Complementation of $\Delta cheW$ by CheW and CheW- fluorescent fusions.
- Figure 10 Complementation of $\Delta cheV$ by CheV and CheV- fluorescent fusions.
- Figure 11 Complementation of $\Delta cheY$ by CheY- fluorescent fusions.
- Figure 12 Complementation of $\Delta fliM$ by FliM- fluorescent fusions.
- Figure 13 Representative fluorescent images of various fusion proteins expressed in *B. subtilis*.
- Figure 14 Confocal image of wild type *B. subtilis* expressing CheA-EYFP.
- Figure 15 Cell Phenotype Metric.
- Figure 16 Possible EYFP/ECFP clustering patterns.
- Figure 17 An example EYFP emission signal during a CheY-EYFP and FliM-ECFP FRET experiment in *B. subtilis*.

List of Tables

Table 1	Cloned Genes and Translational Fusions Inserted into pHCMC04
Table 2	Markerless Deletions of Wild Type <i>B. subtilis</i> Genes
Table 3	List of Primers Used in this Work

Chapter 1: Introduction

How Do Bacteria Navigate Their Environment?

Many bacteria can sense environmental changes and respond by moving. When they do so in response to chemical stimuli, this is known as “chemotaxis.” These chemical signals typically consist of nutrients such as sugars or amino acids. Other chemicals can provide a warning that toxins are nearby. In a strictly aerobic bacterium like *Bacillus subtilis*, oxygen is also an important signal, stimulating “aerotaxis.” Bacteria need a way to sense these many stimuli and then relay that information to the appropriate motility machinery.

Flagellated bacteria, such as *Escherichia coli* and *Bacillus subtilis*, make use of a complex His-Asp phosphorelay system to convert environmental sensory information into instructions for flagellar rotation (34). These instructions result in “running,” where the cell is propelled in one direction, or “tumbling,” which reorients the cell in preparation for a run in another direction (12, 34). Cells can then alternately tumble and run as instructed by their sensory apparatus. By controlling the relative time spent running versus tumbling, a bacterial cell can migrate along chemical gradients and toward more favorable environments (34).

The Mechanics of Chemotaxis Signaling

The bacterial chemotaxis signaling system transmits environmental information across the membrane and relays it to the flagellar motor (see Figure 1). This process begins when the transmembrane receptor protein becomes activated by an external

stimulus and transmits that signal to a protein kinase (CheA) located just inside the membrane (34). CheA then autophosphorylates a conserved histidine residue (12). This phosphate then passes to an aspartate side chain of CheY, the response regulator responsible for changing the rotational direction of the flagellar motor (12). This sensory pathway can be characterized as a His-Asp phosphorelay system, or HAP (41).

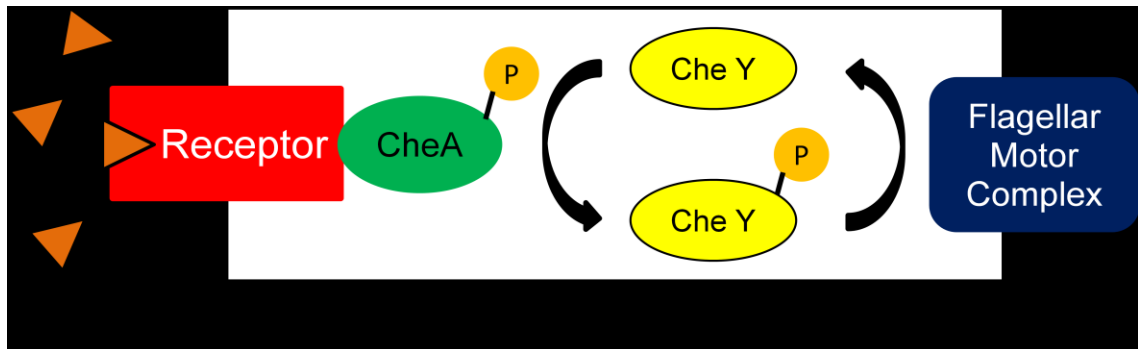


Figure 1: A cartoon of the primary components in the *B. subtilis* chemotaxis circuit.

This HAP pathway differs from traditional two-component signaling systems in several significant ways. First, the role of protein kinase and membrane receptor is usually handled by one molecule instead of the two seen here (12). Second, response regulators most commonly bind to DNA after phosphorylation, either initiating or impeding transcription (12); CheY has neither of these functions. In addition, the chemotaxis signaling system makes use of a core set of proteins (the number of core proteins varying between different bacterial species) (12). For these reasons, “HAP” is a more specific and accurate nomenclature for these chemotaxis signaling proteins and will be used in this thesis rather than “two-component signal transduction.”

Interest in HAP signaling is not limited to basic research. HAP’s are one of nature’s most ancient control mechanisms. While many bacteria require such a system for chemotaxis, analogous signaling systems are widely used to control gene expression,

virulence factors, and biofilm formation (14, 20). Also, many pathogens, such as *Helicobacter pylori* and *Pseudomonas aeruginosa*, require a functional chemotaxis system for virulence (13, 26, 43). It is hoped that characterizing representative model systems will enable a better understanding of species that pose real-world problems.

Why Do We Study *B. subtilis* Chemotaxis?

The largest body of work to date on bacterial chemotaxis regulation has been done in *E. coli*. While this Gram-negative model has laid the foundation for our understanding of chemotaxis signaling, it may only provide limited information about how other bacteria accomplish this same signaling. Due to its highly specific niche in the human gut, it seems to have lost a number of accessory proteins and receptors that still remain in many other species (6).

B. subtilis, on the other hand, contains a copy of every chemotaxis protein so far discovered, excluding *E. coli*'s phosphatase CheZ (37). It is thought that this is because *B. subtilis*' chemotaxis mechanism is more closely related to the ancestral motility mechanism that predates modern Bacteria and Archaea (37). Studying *B. subtilis*, in addition to *E. coli*, may provide a more representative model for chemotaxis signaling in the broad lineage of bacteria.

Several significant components of the *B. subtilis* chemotaxis system are not found in *E. coli*. For example, in *E. coli*, CheY is dephosphorylated by CheZ and this activity does not seem to be regulated by input from either the membrane receptors or the flagellar motor (37). In *B. subtilis*, however, there is no CheZ homolog. Instead dephosphorylation of CheY is accomplished by flagellar protein FliY and phosphatase

CheC. There is evidence that this phosphatase activity may be subject to regulation by the chemoreceptors (3, 23).

Also, alternative coupling protein CheV (discussed in detail later), is not found in *E. coli*, but homologues are found in many medically relevant organisms such as *Helicobacter pylori*, *Salmonella typhimurium*, *Campylobacter jejuni*, as well as *B. subtilis* (1, 19).

While some elements of HAP system organization in *B. subtilis* and other non-*E. coli* bacteria are not fully understood, a larger mystery surrounds possible differences in how the chemotaxis signaling clusters are organized within different bacteria. *E. coli*'s signal clusters seem to congregate most densely at the poles of the cell (44). In contrast *B. subtilis* signal clusters have been observed in a variety of locations: polar, lateral, or both polar and lateral (44).

In addition to variation in signal cluster locations among different bacteria, those signal clusters may also vary in their tendency for dynamic behavior. Some results indicate that *B. subtilis* chemotaxis signal clusters are dynamic, shifting their composition and position in response to attractant stimulation (44). By contrast, *E. coli* signal clusters largely remain in their polar organization, regardless of stimulation (40, 44). Some *E. coli* chemotaxis proteins have been shown to move in and out of signal clusters, but only on a timescale synonymous with adaptation to saturating conditions, not rapid HAP signaling (29).

Practically speaking, *B. subtilis* is already a well-established Gram-positive model organism. It can be cultivated easily in the laboratory and is naturally competent, making it the ideal candidate for complex genetic manipulation. Another advantage of *B. subtilis*

is the wealth of information available about the cytoskeleton and other cell components involved in localizing proteins (5). In theory, this machinery might play an important role in localizing the chemotaxis signaling machinery, a possibility that could be tested by assembling an appropriate “tool box” of mutants and fluorescent fusion proteins (28).

The Genomic Organization of *B. subtilis* Chemotaxis Genes

The flagellar and chemotactic genes in *B. subtilis* are organized into a large operon comprised of 31 genes and spanning almost 27 kilobases (see Figure 2).

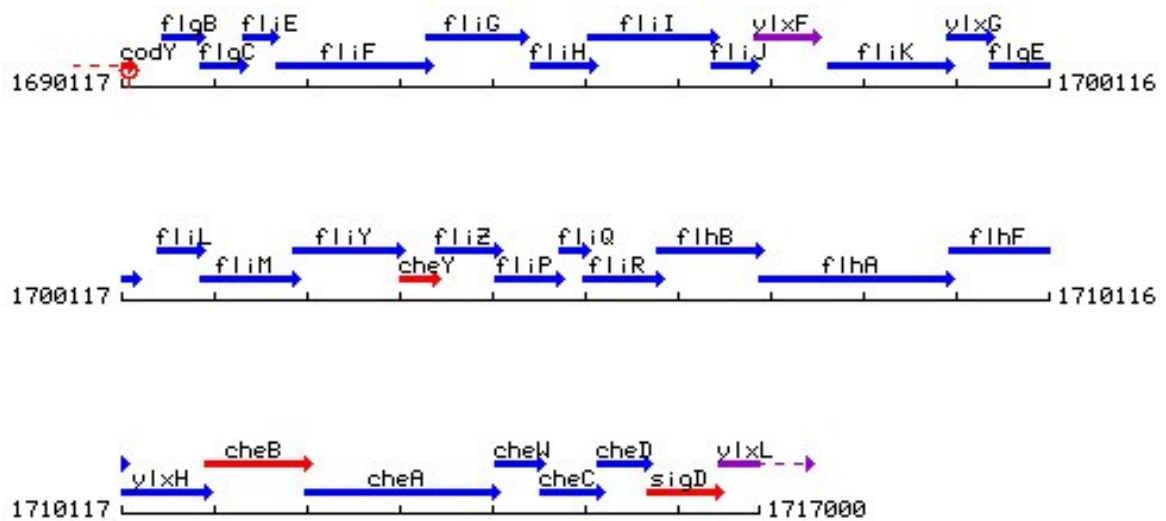


Figure 2: Organization of the *fla/che* operon. Each bar-and-arrow shown represents a gene in the *B. subtilis* 168 genome. The three rows connect from top to bottom, end to end. The operon begins with *flgB* and ends with *ylxL*. Image generated by SubtiList, found at <http://genolist.pasteur.fr/SubtiList/>. Underlying work by Moszer, I., *et al.* (21, 22).

Together this co-transcribed group of genes encode the components of the hook-basal body complex, a number of chemotaxis proteins (including those relevant to this work), and an alternate sigma factor, σ^D (42). In such a highly organized operon, which is responsible for much of the flagellar assembly process (38), one must be careful not to

disrupt operon function when making interior deletions or insertions. For this reason, the site-directed mutagenesis described in Chapter 2 is a markerless deletion system, removing its antibiotic resistance cassette with minimal scarring after homologous recombination has occurred.

The Current Model for *B. subtilis* Chemotaxis Signaling

Explaining the current model for *B. subtilis* chemotaxis signal transduction is best done by first following the route of the primary signal (see Figure 3), then doubling back and revisiting sites where secondary/regulatory processes occur. First, an attractant binds to the methyl-accepting chemotaxis receptor, or MCP, which spans the cytoplasmic membrane (37). The binding occurs in the protein's periplasmic sensory region. Then the signal is transferred across the membrane as a result of conformational changes in the transmembrane helices and the HAMP region of the MCP. Ultimately this generates a change in the conformation of the cytoplasmic signaling region of the MCP (37).

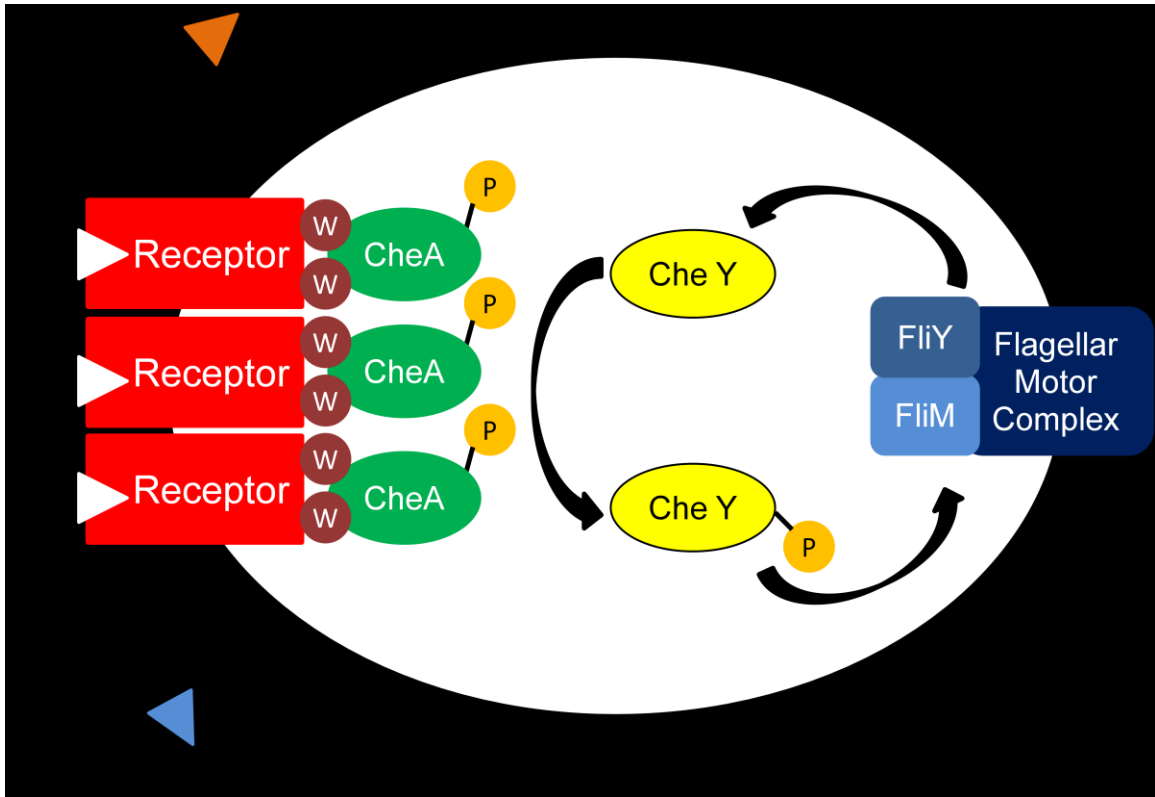


Figure 3: A more detailed model of the *B. subtilis* chemotaxis signaling circuit. The CheA ovals are intended to represent homodimers and the Receptor rectangles are intended to represent numerous dimers assembled into a dense signal cluster. Membrane receptors and CheA are coupled by CheW molecules (in homodimers, as shown). The ball-and-stick P's are meant to indicate bound phosphates.

The MCP signaling region then propagates the signal to CheA, resulting in a dramatic increase in its autokinase activity (37). This kinase activity modulation takes place in the context of large, multi-protein complexes that include receptor proteins, CheA, and CheW, a coupling protein. In one popular *E. coli* model, the minimal signaling complex includes 6 receptor protein molecules (a trimer of dimers), two CheA molecules (a dimer), and two molecules of CheW (37, 41). Stoichiometries of *B. subtilis* CheA and CheW molecules align closely with those of *E. coli*, suggesting that its cytoplasmic complex may be similarly structured (6). No detailed analysis has been done to determine the composition of the transmembrane receptor complex in *B. subtilis*, but the ratio of membrane receptor molecules to CheA molecules in *B. subtilis* is much higher than in *E. coli* (6). *B. subtilis* is known to have many more membrane receptors than *E. coli*, many of these being oxygen receptors, but this stoichiometry also allows for the possibility that *B. subtilis* receptor protein arrangement differs significantly from the *E. coli* model (6, 44).

Once CheA-P has formed, the phosphate can be transferred to CheY to form CheY-P (37). In *B. subtilis*, attractants cause CheA kinase activity to increase and CheY-P causes counter clock-wise (CCW) rotation once it interacts with FliM, a switch protein located on the base of the flagellar rotor (37). When the flagella are all turning CCW, the individual filaments form a bundle that propels the cell in a unidirectional run (39). If a number of the flagella begin to turn CW, the bundle separates and the cell will tumble until the flagella can once again reach a consensus (39). In short, attractants stimulate running behavior and their absence stimulates tumbling behavior.

What Are the Mechanisms of Signal Adaptation in *B. subtilis*?

One aspect of the *B. subtilis* chemotaxis system that diverges significantly from the *E. coli* model is its sensory adaptation system. Adaptation allows a system to become desensitized to a specific stimulus, enabling the system to detect a chemical gradient and seek out a better environment, even in the presence of low levels of that same stimulus (16, 23).

Adaptation in *B. subtilis* can occur by way of several mechanisms: dephosphorylation of the response regulator, methylation of the membrane receptor, or, potentially, the phosphorylation of CheV (16).

Dephosphorylation of CheY-P is the primary regulation method for signals that have already passed through the receptor complex (23). While CheZ is responsible for this in *E. coli*, *B. subtilis* contains several proteins thought to be CheY-P phosphatases, namely FliY and CheC (see Figure 4) (23).

FliY, a part of the flagellar motor complex, has strong phosphatase activity, converting CheY-P to CheY (36). This promotes the central stimulation circuit: CheY-P stimulates FliM to change the direction of flagellar rotation and the phosphate is subsequently stripped off by FliY.

Ordinarily CheC has comparatively weak phosphatase activity (23, 36), but in the presence of receptor deamidase CheD, CheC increases its phosphatase activity 5-fold, returning the system to pre-stimulatory levels of CheY-P (23, 36).

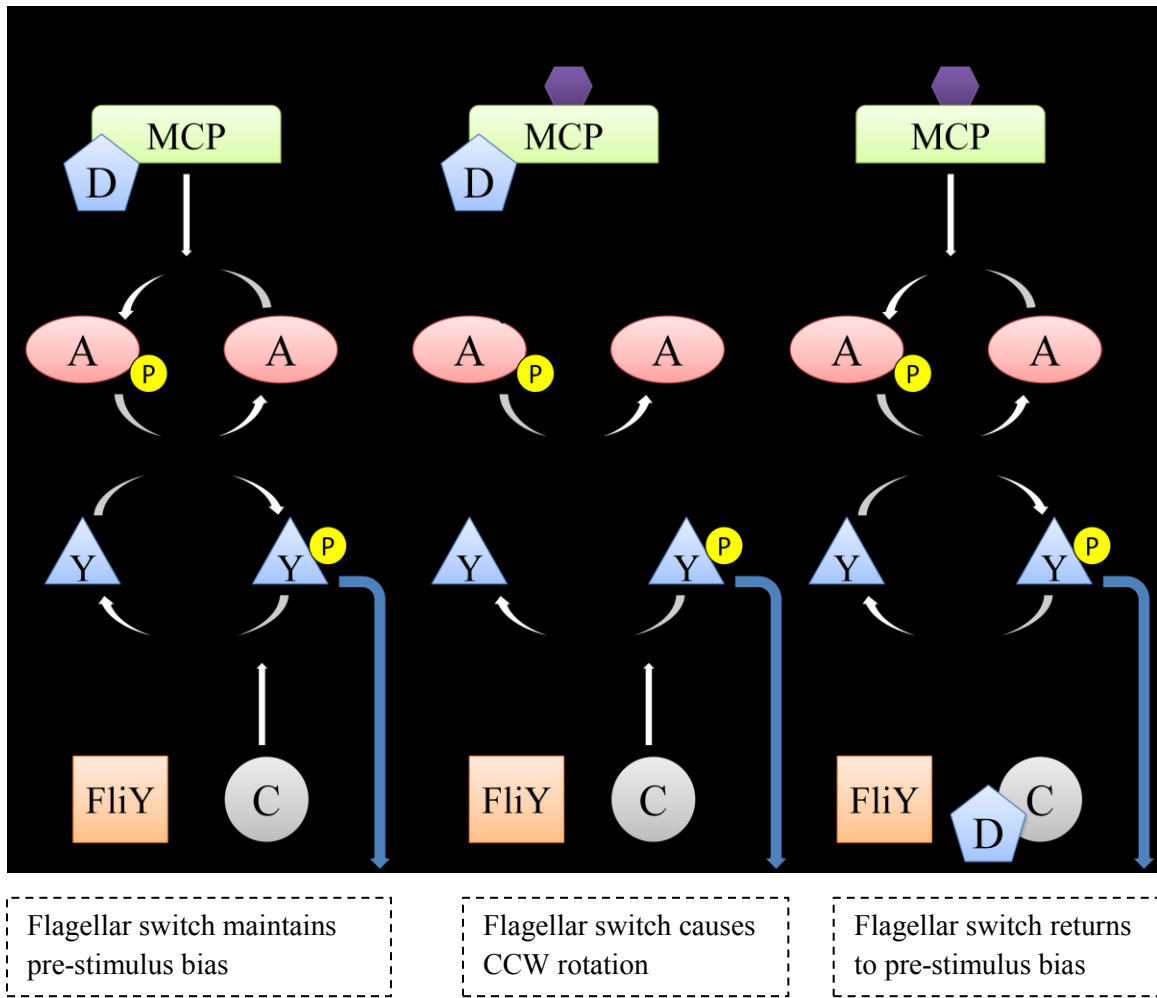


Figure 4: Step-wise model for stimulation and adaptation. Before stimulation (left), CheA autophosphorylation levels are low and FliY acts as a strong phosphatase. After the MCP is excited by an attractant (center), CheA autophosphorylation activity increases and CheY-P levels also increase, generating a CCW “run” signal. The adaptation step (right) occurs when CheD leaves the receptor and binds to CheC. This dramatically increases CheC phosphatase activity and returns the CheY-P concentration to pre-stimulatory levels. Figure based on an image from Muff and Ordal, *J Biol Chem*, 2007.

CheR and CheB reversibly methylate and demethylate glutamate residues of the MCP, respectively (3). As methylation reduces the receptor's binding affinity for attractants, this serves as another form of adaptation. While its role in methylation-dependent adaptation is not well understood, CheD also deamidates the glutamine residues of the MCP into glutamates, a precursor to methylation by CheR (23, 36).

An alternative coupling protein, CheV, has received some attention in recent years for its role in both signal complex organization and sensory adaptation. As a coupling protein, it seems to be able to function in place of CheW, the traditional coupling protein, by bringing the MCP and CheA into contact (by way of a CheW-like domain, see Figure 5). Cells deficient in either CheW or CheV can still carry out chemotaxis, but cells deficient in both proteins cannot (27). There is evidence that CheW may be important for clustering at the poles and CheV for clustering along the sides of the cell (44).



Figure 5: A cartoon diagram of *cheV* in *B. subtilis*. Most notably, the gene contains both a CheW-like domain and a CheY-like domain (10). The former allows for receptor-kinase coupling and the latter allows CheV to accept a phosphate from CheA-P. Figure based on an image from Fredrick and Helmann, *J Bacteriol*, 1994.

Aside from its function as a coupling protein, CheV is involved in adaptation. By way of a CheY-like domain (see Figure 5), CheV can accept a phosphate from CheA-P, though at a much slower rate than CheY (16). This “phosphate sink” activity suggests

that CheV may help stabilize pre-stimulatory CheY-P levels, but will not interfere significantly with CheY-P levels during stimulation (16). It is unclear at this time whether CheV merely absorbs phosphates from CheA to maintain pre-stimulatory equilibrium or CheV requires phosphorylation to carry out all of its functions (16). Strains containing CheV mutants incapable of phosphorylation could still respond to stimulation (attractants and repellents), but had almost no ability to adapt to chemotaxis stimuli (16).

Studying the fine points of *B. subtilis* adaptation may shed light on how other bacteria regulate information from environmental stimuli. It will also grow our overall understanding of the signal adaptation phenomenon, a ubiquitous mechanism found across every biological kingdom.

Comparing Methods for Labeling Intracellular Proteins

The long-term goals for this program of research are to understand not only the spatial arrangement of *Bacillus subtilis* chemotaxis signaling proteins, but also to determine how that arrangement affects chemotaxis behavior. The work in this thesis attempts to characterize how the proteins are arranged and to develop workable strains with which to further study protein function.

A very popular method for labeling proteins, within the context of the cell architecture, is fluorescent localization. As fluorescent dyes do not easily penetrate the bacterial cell membrane, researchers have developed two methods for attaching a fluorescent marker to an intracellular protein of interest.

One method is immunofluorescence imaging. Cells expressing a native version of the protein of interest are fixed to a slide and permeabilized. A primary antibody, specific to the protein of interest, is then applied. Once attached, a secondary antibody conjugated to a fluorophore (such as FITC) is then bound to the primary antibody (44). The sample can then be excited with light and localization points can be observed.

This method has been used for numerous localization experiments, including those investigating chemotaxis proteins (31, 44). It was useful in identifying the independent locations (polar or lateral clustering) of coupling proteins CheW and CheV in the cell structure.

Immunofluorescence is often favored because it introduces no mutations into the bacterial chromosome, so proteins travel to their native locations prior to labeling. However, there are two downsides to this method, within the context of membrane protein localization. First, the cells die once they are permeabilized and cannot be observed in real-time. Cells can be stimulated and then rapidly fixed, but shifts among protein clusters might happen faster than the relatively slow fixing process. Also, the process of permeabilizing the membrane might damage the native arrangement of receptor complexes.

As an alternative to immunofluorescence, experimenters have engineered translational fusions that connect the gene of interest to a gene encoding green fluorescent protein (or any analogous colored fluorophore). Live cells expressing these fluorescent fusion proteins are then observed directly under fluorescence microscopy (31). This technique allows observation of cells in real-time as they react to new

chemical environments. Also, quite a few experiments can be crafted around these genetically modified strains.

Förster resonance energy transfer (FRET) is one option for live cell measurement. This technique uses pairs of translational fluorescent fusions to measure protein-protein interactions. Each pair consists of one “donor” fusion protein and one “acceptor” fusion protein. Often, cyan fluorescent protein (CFP) is the donor, emitting a cyan signal when excited by the experimenter. If a yellow fluorescent protein (YFP) is within a few nanometers of the excited CFP, then some of the energy from the CFP emission is transferred to YFP and a yellow signal is also emitted. With this binary signaling system, pairs of proteins each fused to one of the fluorophores can be said to be interacting when a yellow signal is received (30, 32).

Another useful live-cell method used extensively in both chemotaxis and cytoskeleton structure research is fluorescence recovery after photobleaching (FRAP) (7, 29). It allows researchers to identify whether new tagged proteins have entered a previously photobleached area. FRAP has been used in studying *E. coli* response regulator turnover and adaptation dynamics (29). In *B. subtilis* chemotaxis studies, it could be used to identify at what rate adaptation causes signal clusters to reorganize.

The disadvantage of live cell fluorescence studies lies in the fusion proteins, which may not fold properly and/or not be directed to their native positions within the cell cytoskeleton. This worry can be lessened when studying a chemotaxis system by comparing the function of the mutant proteins to their wild type counterparts. Both the ability to traverse motility agar and the tumble/run frequency of individual cells can be quantified as a way of qualifying mutant proteins. Since the locations of some proteins

have been tied to their function (44), it is likely that a mutant strain that functions like wild type is also localizing correctly. Another way to confirm like-wild type function is to compare native protein immunofluorescence localization to that of the mutant protein.

Both immunofluorescence and translational fusion imaging have their advantages and drawbacks. It appears that analyzing the same system with both methods would strengthen any findings and mitigate many concerns about experimental design.

Chapter 2: Experimental Methods

PCR Cloning and Bacterial Transformation

The initial focus of the work was to develop a number of translational fluorescent fusions and localize the core Che/Fli proteins. This began by cloning *che/fli* genes of interest (see Table 1) from wild type chromosomal DNA by polymerase chain reaction (PCR) cloning (see Table 3 for primers used). Each gene was modified by its primers to include a six glycine codon sequence on one end. These fragments were subsequently inserted into a TOPO vector (pCR-Blunt, Invitrogen) and transformed into *E. coli* (DH5- α).

The steps above were repeated, but after initial PCR amplification, overlap PCR was used to fuse the gene of interest to an *eyfp* or *ecfp* (Clontech) fragment also containing a complementary glycine codon sequence. This “linker” sequence was designed to allow for a full range of motion between the two protein partners after translation. *eyfp*-“gene” and “gene”-*eyfp* orientation of each fusion were created in case one orientation impeded the normal functions of the native protein component.

Once completed, the fragments were purified and ligated into pHCMC04, an *E. coli/B. subtilis* shuttle vector (see Figure 6) (24). pHCMC04 controls expression of genes inserted into its multiple cloning site by way of a xylose-inducible promoter (P_{xyl}). In the *B. subtilis* 168 chromosome, this promoter is used to regulate transcription of xylose catabolism genes (*xylAB*) by way of a repressor (XylR), which blocks P_{xyl} from functioning in the absence of xylose (24). In pHCMC04, both P_{xyl} and *xylR* have been included to replicate this regulatory relationship artificially (see Figure 6).

All of the cloned genes (and their fusions) developed so far are listed in Table 1. All of the plasmid constructs in Table 1 were then transformed into wild type *B. subtilis* (OI1085) as well as the appropriate deletion strains (see Table 2 and Figures 8-12).

Table 1: Cloned Genes and Translational Fusions Inserted into pHCMC04

<i>cheA</i>	<i>cheW</i>	<i>cheV</i>		
<i>cheA-eyfp</i>	<i>cheW-eyfp</i>	<i>cheV-ecfp</i>	<i>cheY-eyfp</i>	<i>fliM-ecfp</i>
<i>eyfp-cheA</i>	<i>eyfp-cheW</i>	<i>ecfp-cheV</i>	<i>eyfp-cheY</i>	<i>ecfp-fliM</i>

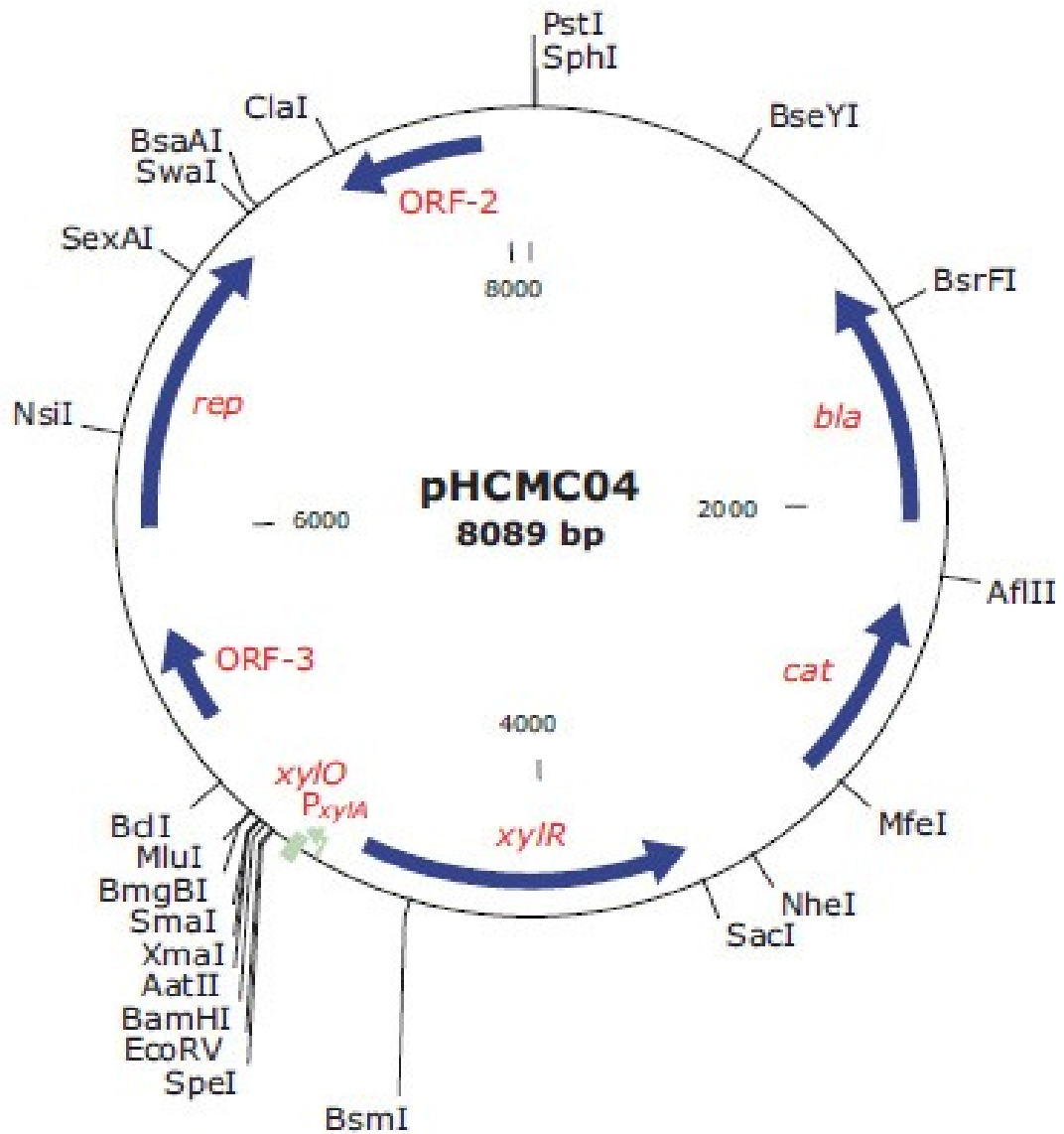


Figure 6: Plasmid map of pHCMC04. Components of note: *bla* (conferring ampicillin resistance), *cat* (conferring chloramphenicol resistance), *xyIR* (a repressor of P_{xyIA}), and P_{xyIA} (a xylose-inducible promoter). Plasmid developed by Nguyen, H. D., *et al.* in *Plasmid*, 2005. Image from the Bacillus Genetic Stock Center (www.bgsc.org).

Site-Directed Mutagenesis

To create markerless deletions of *che/fli* genes in the *B. subtilis* chromosome, I employed a method referred to as the “Xer-cise” method (4). To create each deletion strain, I transformed *B. subtilis* with a linear vector that causes a homologous crossover event on either side of the gene of interest. The vector then transfers the gene of interest to the linear vector, which is degraded, and inserts into the chromosome a chloramphenicol resistance cassette (CAT) flanked by two identical “dif” sites. These dif sites subsequently signal the cell’s innate Xer machinery, normally responsible for resolving plasmid and chromosomal dimers, to excise the CAT marker, leaving a single dif site in place of the deleted gene. This ultimately leaves a stable markerless deletion and can be arranged as so not to disturb surrounding genes within the same operon (4).

The linear vector for Xer-cise was constructed from a pCR4 TOPO vector (Invitrogen) into which the difCAT construct had been inserted. On either side of the difCAT, a region of sequence was inserted to mimic the sequence directly upstream and downstream of the gene of interest. These “flank” sequences were amplified from *B. subtilis* 1A1 genomic template PCR (for primers, see Table 3) and were engineered to contain the first and last three codons of the deleted gene (to protect operon structure and provide a buffer for downstream ribosomal binding sites). After the flanks were inserted, the entire construct (pictured in Figure 7) was digested out of pCR4 TOPO and transformed into *B. subtilis*, which readily takes up linear DNA.



Figure 7: Template for Xer-cise deletion construct.

After selection on chloramphenicol plate media, I restreaked on non-selective media until the transformants showed sensitivity to chloramphenicol. Chromosomal DNA was isolated from these strains (using GenElute™ Bacterial Genomic DNA Kit, Sigma-Aldrich) and used as template DNA for PCR reactions to confirm the presence of intended deletions. Thus far I have developed five markerless deletion strains in *B. subtilis*, shown in Table 2.

Table 2: Markerless Deletions of Wild Type *B. subtilis* Genes

$\Delta cheA$	$\Delta cheW$	$\Delta cheV$	$\Delta cheY$	$\Delta fliM$
---------------	---------------	---------------	---------------	---------------

Motility Agar Assays

In order to measure the different chemotaxis phenotypes of *B. subtilis* strains, I followed a standard protocol to test the ability of a strain to traverse a plate of semi-liquid media. Aliquots of saturated liquid cultures (from LB media tubes with 5 µg/mL chloramphenicol shaken overnight) were used to inoculate motility agar plates (Bacto agar, tryptone, NaCl, and 5 µg/mL chloramphenicol) (39). Plates were each inoculated with bacteria containing a variant of pHCMC04 and contained an appropriate concentration of xylose for the purpose of induction (plates used to grow uninduced cultures were volume balanced with sterile ddH₂O). Plates were then be incubated for 10-12 hours at 30°C (a vessel of water was placed under the plates to reduce plate dehydration). The diameter of the *B. subtilis* colony on each plate was then measured to gauge relative chemotaxis ability. These assays were performed in triplicate and the swim zone diameters were subsequently averaged. The statistical significance of the apparent differences between any two of these averages was determined by applying Student's *t*-test (two-tail), assuming unequal variances, to the sets of sample

measurements comprising each average. p values of ≤ 0.05 were considered to indicate that the difference between two sets of sample data was statistically significant.

Fluorescence Microscopy

The fluorescent fusion transformants were imaged under wide-field fluorescence microscopy using a Nikon 80i instrument and samples on glass slides at room temperature. Slides were either prepared as traditional wet mounts or with broth cultures spotted onto 0.2% agarose pads. The latter preparation helped the cells remain longitudinally in plane during imaging. Bacterial samples were either extracted from the outer rings of a motility agar plate or simply taken from an overnight broth culture (shaken at ~ 250 rpm at 37°C). Both the motility agar and the broth contained $5\mu\text{g/ml}$ chloramphenicol and optimal concentrations of xylose inducer, as determined by viewing images of varying inducer concentrations. For viewing YFP fusions, a Nikon C-FI YFP HC HISN Zero Shift filter cube was used. For viewing CFP fusions, the filter cube was a Nikon C-FL CFP HC HISN Zero Shift. Images displayed in this thesis were collected using a 100X oil immersion lens (CFi Plan APO DM 100X) and a 10X ocular lens for a total magnification of 1000X. Images were captured using NIS-Elements software and a DS-QI1 digital camera.

Chapter 3: Results and Discussion

At the outset of this project, one of my main goals was to examine the spatial arrangement of *Bacillus subtilis* chemotaxis signaling proteins in living cells. My strategy was to create translational fusions between chemotaxis genes and *eyfp* (or *ecfp*). To examine the location and functionality of the encoded fusions, I wanted to express each of these fusions in a *B. subtilis* strain from which the corresponding normal copy of the chemotaxis gene had been deleted (individually). This required that I first create these deletions strains. The Xer-cise method for site-directed mutagenesis was chosen because it leaves behind only a small “scar” region in the genome after a successful deletion (4), hopefully minimizing polar effects in the gene’s operon.

Below I describe my efforts to create a standardized set of markerless single-gene deletion strains and my initial characterization of these strains. Then I describe my analysis of the ability of each chemotaxis fusion protein to restore chemotaxis ability in the deletion strains.

Developing a *cheA* Deletion Strain

I chose CheA as a target for investigation because its autophosphorylation rate directly determines how much CheY-P will be available to interact with the flagellar switch protein, FliM. Also, CheA has been tracked previously in the *E. coli* model to indicate the location of chemotaxis signal clusters along the cell membrane (31).

Using the Xer-cise method (4), *cheA* was deleted from the *B. subtilis* genome, leaving behind only a “scar” region. This deletion was confirmed by a PCR reaction

containing isolated chromosomal DNA from the mutant strain, primer XerALFU_p, and primer XerDnARF (from Table 3). A control reaction was set up with the same primers and OI1085 wild type chromosomal DNA. After electrophoretic analysis on a 0.9% agarose gel, the amplified fragment from the mutant DNA was found to be approximately 2000bp shorter than the wild type fragment, a size equivalent to the length of *cheA*.

Next, the $\Delta cheA$ strain was grown on motility agar at 30°C. As seen in Figure 8, the $\Delta cheA$ strain performed dramatically worse than the wild type strain. This swimming phenotype matches the expected *che*⁻ phenotype seen in previous work by the Ordal research group (11, 12).

To complement the deletion with a copy of the native gene, pHCMC04::*cheA* was transformed into the $\Delta cheA$ strain. In the motility plate assay (see Figure 8), expression of the native protein was only able to restore function to about half of wild type. Function did improve slightly in a greater concentration of inducer, so it is possible that more protein expression is necessary to rescue the chemotaxis phenotype.

Design and Characterization of *cheA* Translational Fusions

A translational fusion of *cheA* and *eyfp* was developed as described in the methods, generating two fusion orientations. Each fusion was individually inserted into the plasmid pHCMC04. This plasmid was then transformed into the $\Delta cheA$ strain.

The $\Delta cheA$ strain (pHCMC04::*cheA-eyfp* and pHCMC04::*eyfp-cheA*) was compared to both the wild type strain (empty vector) and the $\Delta cheA$ strain (empty vector) in a motility agar plate assay in the presence of varying concentrations of xylose (see Figure 8). Both fusions performed better than the $\Delta cheA$ strain (empty vector), but only

the *eyfp-cheA* performed as well as the native *cheA* gene in restoring chemotaxis function. The lack of a full rescue of the phenotype is likely either due to insufficient production of protein or an undiscovered polar effect from the gene deletion.

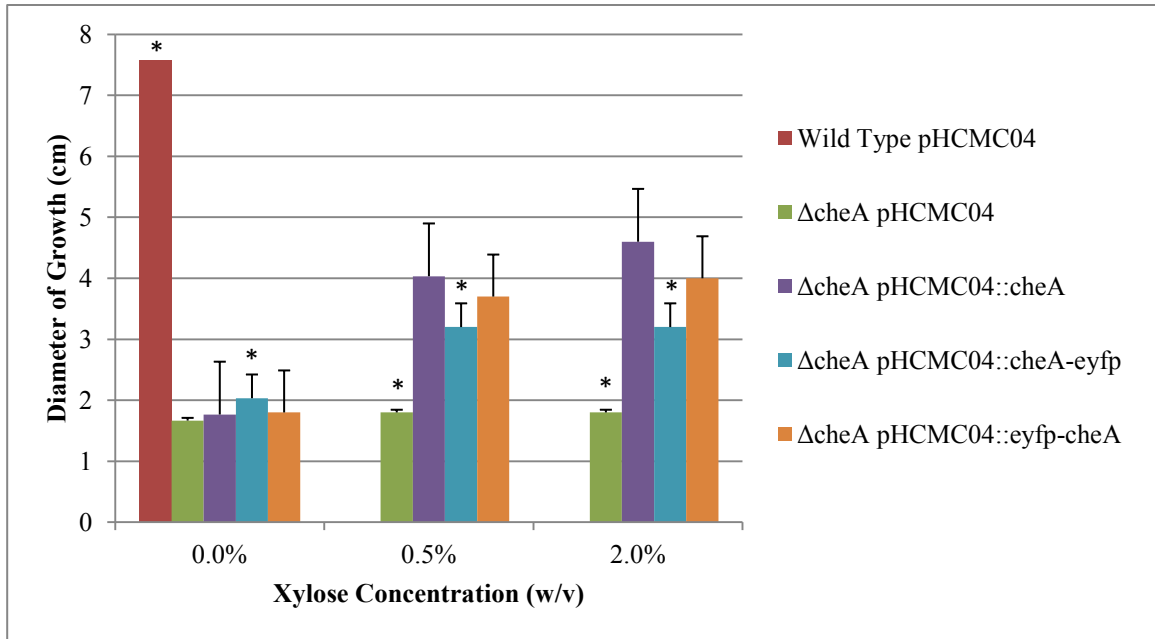


Figure 8: Complementation of $\Delta cheA$ by CheA and CheA- fluorescent fusions.

Empty vector strains of wild type and $\Delta cheA$ were compared to $\Delta cheA$ strains expressing native CheA or CheA- fluorescent fusions (two orientations). All data bars represent the average of three replicate plates. Error bars represent standard error.

An * in the 0.0% grouping indicates a significant difference from the $\Delta cheA$ pHCMC04 strain ($p \leq 0.05$).

An * in the 0.5% grouping indicates a significant difference from the $\Delta cheA$ pHCMC04::cheA strain ($p \leq 0.05$).

An * in the 2.0% grouping indicates a significant difference from the $\Delta cheA$ pHCMC04::cheA strain ($p \leq 0.05$).

Developing a *cheW* Deletion Strain

I chose CheW as a localization target because of its importance in both signal cluster organization and signal cluster dynamics (37, 41, 44). When paired with the above CheA fluorescent fusions, it may reveal when these two proteins most frequently colocalize. I also believe a CheW fusion would be a useful point of comparison when studying CheV localization and function.

Using the Xer-cise method (4), *cheW* was deleted from the *B. subtilis* genome, leaving behind only a “scar” region. This deletion was confirmed by a PCR reaction containing isolated chromosomal DNA from the mutant strain, primer BsW5up, and primer BsW3dn (from Table 3). A control reaction was set up with the same primers and OI1085 wild type chromosomal DNA. After electrophoretic analysis on a 0.9% agarose gel, the amplified fragment from the mutant DNA was found to be about 500bp shorter than the wild type fragment, a size equivalent to the length of *cheW*.

Next, the $\Delta cheW$ strain was grown on motility agar at 30°C. The $\Delta cheW$ pHCMC04 strain lost a significant portion of its chemotaxis swimming ability (see Figure 9), but could swim well enough to leave the initial point of inoculation, as seen in previous studies (27). This partial maintenance of chemotaxis function is thought to be due to CheV taking over as the primary coupling protein (27).

To complement the deletion with a copy of the native gene, pHCMC04::*cheW* was transformed into the $\Delta cheW$ strain. In the motility plate assay (see Figure 9), expression of the native protein completely restored chemotaxis function in $\Delta cheW$ when induced with even 0.5% xylose. This shows that the deletion is both non-polar and can be easily restored to wild type levels with a feasible level of CheW protein production.

Design and Characterization of *cheW* Translational Fusions

A translational fusion of *cheW* and *eyfp* was developed as described in the methods, generating two fusion orientations. Each fusion was individually inserted into the plasmid pHCMC04. This plasmid was then transformed into the $\Delta cheW$ strain.

The $\Delta cheW$ strain (pHCMC04::*cheW-eyfp* and pHCMC04::*eyfp-cheW*) was compared to both the wild type strain (empty vector) and the $\Delta cheW$ strain (empty vector) in a motility agar plate assay in the presence of varying concentrations of xylose (see Figure 9). Both orientations of the CheW-EYFP fusion were able to rescue the phenotype of the knockout with slightly higher (2.0%) levels of inducer. While it is still unknown whether these fusions replicate all behaviors of the native protein, these data show that the cell can use both fusions effectively in receptor-kinase coupling.

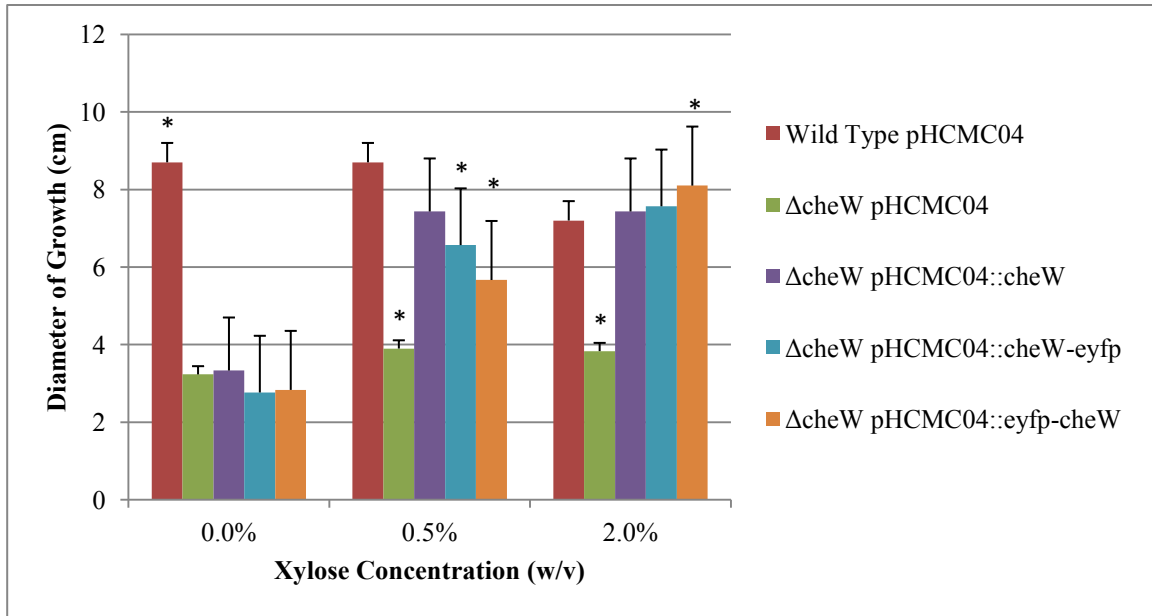


Figure 9: Complementation of $\Delta cheW$ by CheW and CheW- fluorescent fusions.

Empty vector strains of wild type and $\Delta cheW$ were compared to $\Delta cheW$ strains expressing native CheW or CheW- fluorescent fusions (two orientations). All data bars represent the average of three replicate plates. Error bars represent standard error.

Plates for $\Delta cheW$ pHCMC04::eyfp-cheW (0.5% xylose) and Wild Type pHCMC04 (2.0% xylose) were made in a separate batch from other samples in this figure, but were incubated under similar conditions.

Growth in some of the Wild Type pHCMC04 (0.0% and 0.5% xylose) plates reached the lip of the Petri dish before measurements could be taken.

An * in the 0.0% grouping indicates a significant difference from the $\Delta cheW$ pHCMC04 strain ($p \leq 0.05$).

An * in the 0.5% grouping indicates a significant difference from the Wild Type pHCMC04 strain ($p \leq 0.05$).

An * in the 2.0% grouping indicates a significant difference from the Wild Type pHCMC04 strain ($p \leq 0.05$).

Developing a *cheV* Deletion Strain

I chose CheV as a localization target because its roles in both receptor-kinase coupling and adaptation to stimulus are not well understood. It would probably be instructive to compare CheV localization patterns to those of CheW and CheA, as a previous study suggests that both coupling proteins (CheW and CheV) are dynamic, shifting between the poles and the long sides of the cell (44), but it is unknown how that reorganization interacts with the position of CheA in the cell.

Using the Xer-cise method (4), *cheV* was deleted from the *B. subtilis* genome, leaving behind only a “scar” region. This deletion was confirmed by a PCR reaction containing isolated chromosomal DNA from the mutant strain, primer BsV5up, and primer BsV3dn (from Table 3). A control reaction was set up with the same primers and OI1085 wild type chromosomal DNA. After electrophoretic analysis on a 0.9% agarose gel, the amplified fragment from the mutant DNA was found to be about 900bp shorter than the wild type fragment, a size equivalent to the length of *cheV*.

Next, the $\Delta cheV$ strain was grown on motility agar at 30°C. Much like the $\Delta cheW$ strain, the $\Delta cheV$ strain shows a partial loss of chemotaxis function, but it is still able to migrate away from the inoculation point (see Figure 10). This is likely due to CheW carrying out enough coupling to form some signal clusters (27).

To complement the deletion with a copy of the native gene, pHCMC04::*cheV* was transformed into the $\Delta cheV$ strain. The motility plate assay (see Figure 10) showed that chemotaxis function is very sensitive to CheV expression. At 0% inducer, the likely leaky P_{xyI} promoter allowed for some CheV expression and chemotaxis function improved over that of the deletion strain. The next inducer concentration showed a drop

in function, as did the highest level of inducer. This suggests that either very little CheV protein is necessary to perform its role in the cell (and that excess CheV has a deleterious effect), or that there is a careful stoichiometry between CheV and other chemotaxis protein components. In the case of the latter, an optimal level of induction may exist outside of those tested in this assay.

Design and Characterization of *cheV* Translational Fusions

A translational fusion of *cheV* and *ecfp* was developed as described in the methods, generating two fusion orientations. Each fusion was individually inserted into the plasmid pHCMC04. This plasmid was then transformed into the $\Delta cheV$ strain.

The $\Delta cheV$ strain (pHCMC04::*cheV-ecfp* and pHCMC04::*ecfp-cheV*) was compared to both the wild type strain (empty vector) and the $\Delta cheV$ strain (empty vector) in a motility agar plate assay in the presence of varying concentrations of xylose (see Figure 10). Looking at the two fusions, both varied in their success at rescuing the phenotype. The CheV-ECFP orientation generally outperformed the native protein in improving chemotaxis function and did so the most consistently within this assay. The ECFP-CheV orientation not only failed to improve function beyond the deletion strain's levels, but worsened chemotaxis function in the absence of xylose. A wider range of xylose concentrations could be tried in future motility agar assays, but higher levels than 2.0% would be difficult, as the xylose stock solution cannot be made in higher concentrations than 50% and larger aliquots of xylose solution can disrupt the solidity of the media. One solution to this difficulty might be to increase the concentration of agar in the swim plates, thus allowing for more dilution by sugar solution.

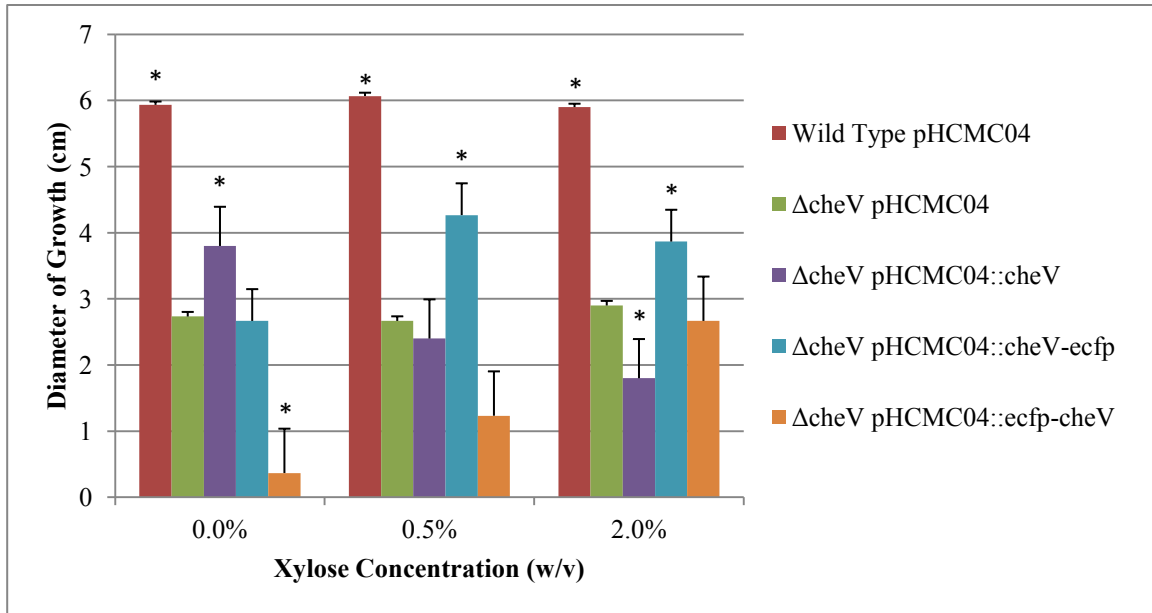


Figure 10: Complementation of $\Delta cheV$ by CheV and CheV- fluorescent fusions. Empty vector strains of wild type and $\Delta cheV$ were compared to $\Delta cheV$ strains expressing native CheV or CheV- fluorescent fusions (two orientations). All data bars represent the average of three replicate plates. Error bars represent standard error.

An * indicates a significant difference from the $\Delta cheV$ pHCMC04 strain in each respective xylose concentration grouping ($p \leq 0.05$).

Developing a *cheY* Deletion Strain

I chose CheY as a target for localization because it has great potential as a colocalization or FRET partner with either CheA, FliM, or any CheY-P phosphatase. Developing a FRET reporter strain to provide feedback about the chemotaxis circuit would be useful, just as it was in the *E. coli* chemotaxis signaling system (18, 33).

Using the Xer-cise method (4), *cheY* was deleted from the *B. subtilis* genome, leaving behind only a “scar” region. This deletion was confirmed by a PCR reaction containing isolated chromosomal DNA from the mutant strain, primer BsY-5up, and primer BsY-3dn (from Table 3). A control reaction was set up with the same primers and OI1085 wild type chromosomal DNA. After electrophoretic analysis on a 0.9% agarose gel, the amplified fragment from the mutant DNA was found to be about 350bp shorter than the wild type fragment, a size equivalent to the length of *cheY*.

Next, the $\Delta cheY$ strain was grown on motility agar at 30°C. As seen in Figure 11, this strain lost all chemotaxis ability and was unable to migrate away from the initial inoculation point. This swimming phenotype matches the expected *che⁻* phenotype seen in previous work by the Ordal research group (12). It should be noted that this swimming distance is significantly smaller than that seen for the $\Delta cheA$ strain (Figure 8). These are chemotaxis signaling partners, so one might expect the defects to be more similar. As discussed in the summary, this discrepancy may be an indicator of a mutation beyond the *cheY* gene.

Unfortunately, I did not manage to develop a plasmid containing the native *cheY* gene in time for the publication of this thesis. In future research, this would be a high

priority to see whether the $\Delta cheY$ strain could be complemented with the native gene and restored to wild type levels of chemotaxis function.

Design and Characterization of *cheY* Translational Fusions

A translational fusion of *cheY* and *eyfp* was developed as described in the methods, generating two fusion orientations. Each fusion was individually inserted into the plasmid pHCMC04. This plasmid was then transformed into the $\Delta cheY$ strain.

The $\Delta cheY$ strain (pHCMC04::*cheY-eyfp* and pHCMC04::*eyfp-cheY*) was compared to the both wild type strain (empty vector) and the $\Delta cheY$ strain (empty vector) in a motility agar plate assay in the presence of varying concentrations of xylose (see Figure 11). Both fusion orientations failed to produce a restoration of chemotaxis function. It is perhaps notable that the CheY-EYFP oriented protein did significantly improve chemotaxis function over the level of the $\Delta cheY$ strain, but this improvement fell far short of the wild type phenotype.

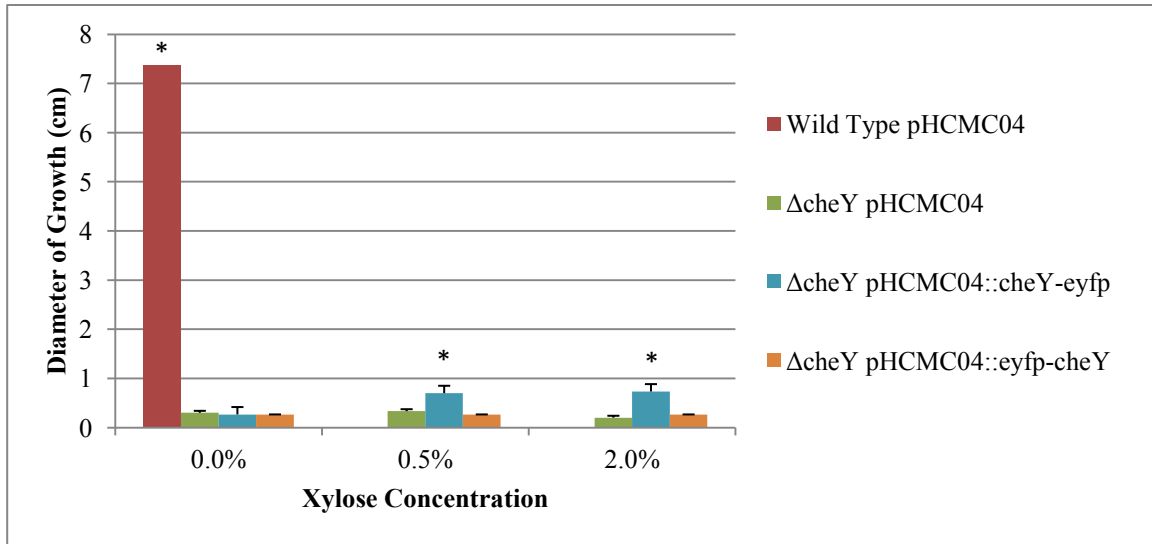


Figure 11: Complementation of $\Delta cheY$ by CheY- fluorescent fusions.

Empty vector strains of wild type and $\Delta cheY$ were compared to $\Delta cheY$ strains expressing CheY- fluorescent fusions (two orientations). All data bars represent the average of three replicate plates. Error bars represent standard error.

An * indicates a significant difference from the $\Delta cheY$ pHCMC04 strain in each respective xylose concentration grouping ($p \leq 0.05$).

Developing a *fliM* Deletion Strain

FliM was chosen as a localization target primarily because it is the flagellar switch protein, and thus the final step in the *B. subtilis* chemotaxis signaling circuit (37). This makes it a useful FRET partner for any fluorescent CheY fusions that can be produced as a result of the above work.

Using the Xer-cise method (4), *fliM* was deleted from the *B. subtilis* genome, leaving behind only a “scar” region. This deletion was confirmed by a PCR reaction containing isolated chromosomal DNA from the mutant strain, primer XerMLFupv2, and primer XerMRFdvn2 (from Table 3). A control reaction was set up with the same primers and OI1085 wild type chromosomal DNA. After electrophoretic analysis on a 0.9% agarose gel, the amplified fragment from the mutant DNA was found to be about 1000bp shorter than the wild type fragment, a size equivalent to the length of *fliM*.

Next, the Δ *fliM* strain was grown on motility agar at 30°C. As seen in Figure 12, this strain lost all chemotaxis ability and was unable to migrate away from the initial inoculation point. This swimming phenotype matches the expected *che*⁻ phenotype seen in previous work by the Ordal research group (35). As mentioned in the section describing the Δ *cheY* strain, these small swimming distances may indicate a mutation to the *fla/che* machinery outside of the *fliM* gene area.

Unfortunately, I did not manage to develop a plasmid containing the native *fliM* gene on it in time for the publication of this thesis. In future research, this would be a high priority to see whether the Δ *fliM* strain could be complemented with the native gene and restored to wild type levels of chemotaxis function.

Design and Characterization of *fliM* Translational Fusions

A translational fusion of *fliM* and *ecfp* was developed as described in the methods, generating two fusion orientations. Each fusion was individually inserted into the plasmid pHCMC04. This plasmid was then transformed into the Δ *fliM* strain.

The Δ *fliM* strain (pHCMC04::*fliM-ecfp* and pHCMC04::*ecfp-fliM*) was compared to both the wild type strain (empty vector) and the Δ *fliM* strain (empty vector) in a motility agar plate assay in the presence of varying concentrations of xylose (see Figure 12). Both fusion orientations failed to provide any improvement to chemotaxis function over the deletion strain. This may be due to the sensitive nature of FliM's structure within the context of the FliNMG ring complex (8). Future constructs might explore modifications to the length of the glycine linker, or alternate methods of fluorescent labeling. Also, without the native protein for comparison it is hard to tell, but one explanation for this result would be a polar effect resulting from the gene deletion process.

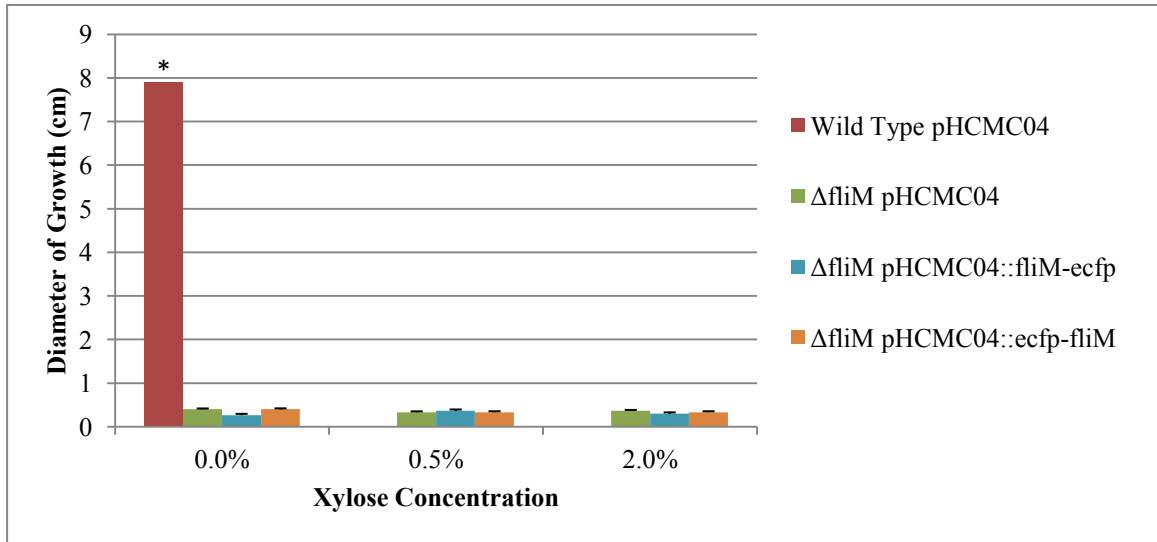


Figure 12: Complementation of Δ fliM by FliM- fluorescent fusions.

Empty vector strains of wild type and Δ fliM were compared to Δ fliM strains expressing FliM- fluorescent fusions (two orientations). All data bars represent the average of three replicate plates. Error bars represent standard error.

Growth in some of the Wild Type pHCMC04 (0.0% xylose) plates reached the lip of the Petri dish before measurements could be taken.

An * indicates a significant difference from the Δ fliM pHCMC04 strain in each respective xylose concentration grouping ($p \leq 0.05$).

Fluorescence Microscopy

While some fluorescent fusion proteins were able to restore chemotaxis function to deficient strains, I also wanted to test overall fluorescence. It was possible that either the eyfp/ecfp subunit of a given fusion might not fold correctly, or might not even be transcribed/translated. Also, I wanted to ensure that the P_{xyl} promoter in pHCMC04 was sufficiently active to produce a microscopically visible level of fluorescence. It was important to see whether fluorescent localization points would form throughout the cell.

All of the strains I imaged were wild type OI1085 transformed with pHCMC04 containing one of the translational fluorescent fusions in Table 1. Figure 13 displays a representative image of each fluorescent fusion (orientation with the clearest localization points). With most of the fusions, the fluorescence images of the bacteria looked very similar: bright spots speckling the length of the cell, often in a repeated, staggered pattern. Typically, different orientations of the same fusion pair looked similar under microscopy, but sometimes one strain was prone to greater brightness and became the preferred candidate for image capture.

Additionally, a series of images were taken with a confocal microscope (Leica) in the CBMG Imaging Core (see Figure 14). The limit of resolution for this microscope was not significantly better than that of the previous microscope. One advantage of this technique, however, was slower photobleaching in the pHCMC04::*cheA-eyfp* transformants I observed. Future experiments requiring a time course measurement or greater excitation energy could benefit from confocal microscopy.

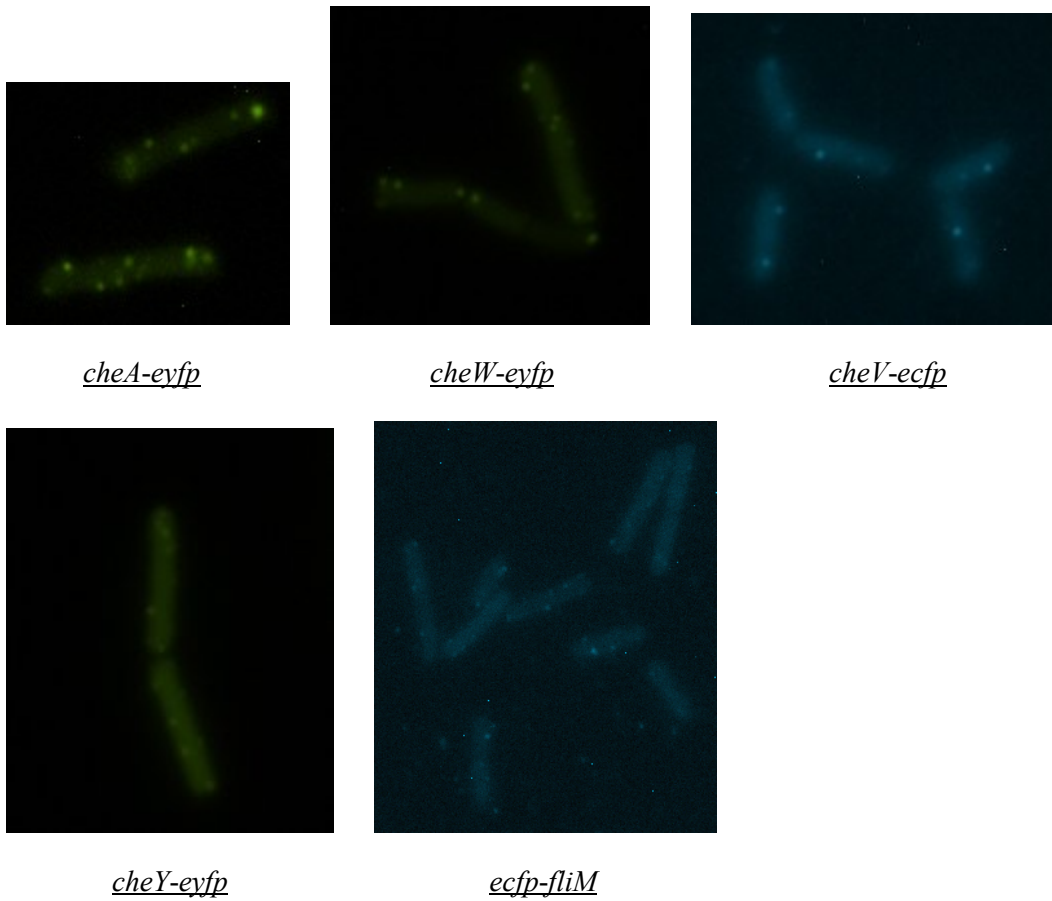


Figure 13: Representative fluorescent images of various fusion proteins expressed in *B. subtilis*.

All images were taken by a wide-field fluorescent microscope at 1000x magnification using a YFP or CFP filter cube. Indicated fusions were expressed using plasmid pHCMC04, transformed into wild type strain OI1085. All images displayed numerous bright spots along the length of the cell.

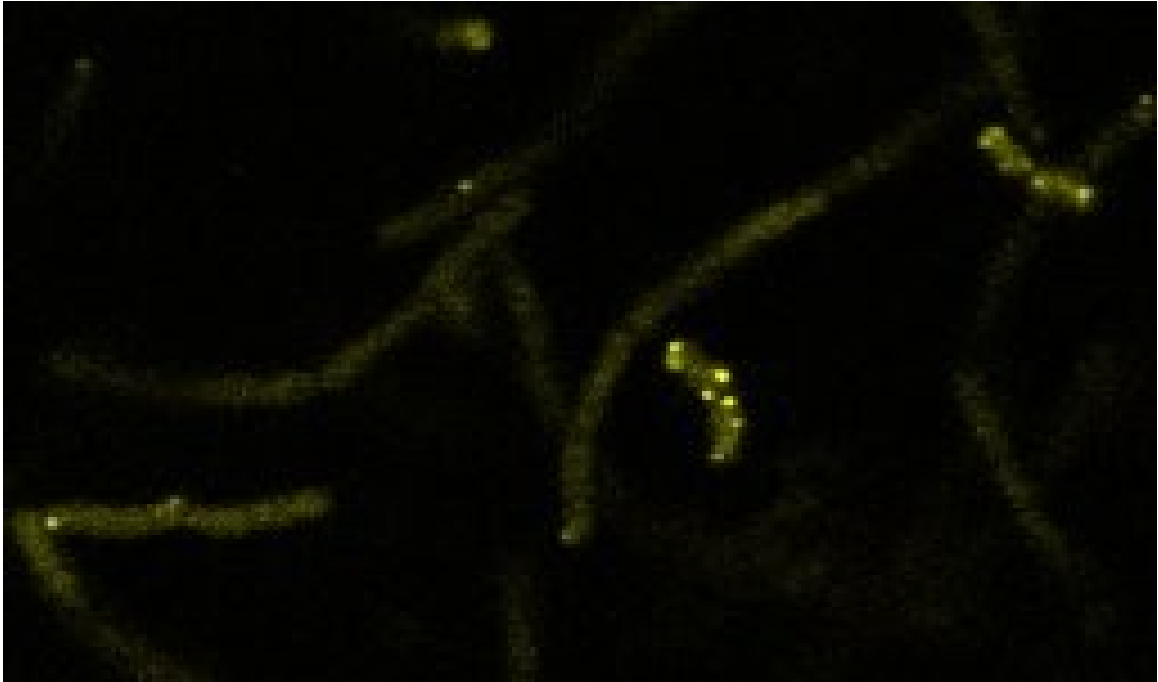


Figure 14: Confocal image of wild type *B. subtilis* expressing CheA-EYFP. Representative image was taken by a Leica SP5 X confocal microscope at 1000x magnification (single image slice). Samples were excited by an argon laser set to a wavelength of 514nm. *cheA-eyfp* was expressed using plasmid pHCMC04, transformed into wild type strain OI1085.

Discussion of Results

Out of the five sets of fusion proteins examined here (all of which demonstrated microscopic fluorescence), three (CheA, CheW, and CheV) demonstrated the ability to restore some chemotaxis function, while two (CheY and FliM) had no impact on their deletion strains.

The CheW fusions were the most successful. The native protein and both fusion orientations performed equivalently and all three proteins were able to rescue the chemotaxis phenotype.

Both the CheA and CheV fusions showed promise in their potential to complement their respective deletion strains, but neither fully restored chemotaxis. Only two xylose induction levels were tested, so it may be that further optimization of induction will bring about better complementation. Both of the native proteins and all but one of the fusions were able to significantly improve chemotactic swimming, so it does look like further troubleshooting is worth pursuing.

The two unsuccessful fusions, CheY and FliM, were also the only two proteins not compared to the appropriate native protein. Unfortunately, the two native gene plasmids could not be prepared in time for the writing of this manuscript. If the two fusions were later compared to their native protein (as with the other three target genes) and they too failed to improve the deletion strain, it might mean that either the plasmid's promoter is insufficient to produce enough protein or that a polar effect resulting from the deletion procedure has disrupted genes neighboring the deletion zone. Conversely, if the native protein performed well, then each fusion would need to be reexamined both structurally as well as genetically, to determine the reason for such disparate results.

It is my opinion that a polar gene disruption is to blame for a lack of phenotype rescue by the fusion proteins. A major clue is the area of growth/swimming. As seen in the CheA motility assay (Figure 8), a *B. subtilis che⁻* mutant should still be able to tumble continuously without any chemotaxis machinery, as this is the natural bias of the flagella. Both the $\Delta cheY$ strain and the $\Delta fliM$ strain were able to grow less than a centimeter in diameter, which makes the case that these strains may not only be non-chemotactic, but also non-motile. This Fla⁻ phenotype can be explained by the relatively upstream location of these two genes within the *fla/che* operon. Unintended disruptions around either of these genes might have lead to cells without functional flagella. Both a wet mount (looking for tumbling) and a flagella stain could be carried out to verify this phenotype.

In order to better qualify all of the fusions for use in future experiments (see Chapter 4), it would be good to know not only how the proteins function in comparison to the native proteins, but also how much of each protein is being produced. Chemotaxis machinery is sensitive to protein-protein stoichiometry (6), so it is likely that function may be the result of not only protein translation and structure, but also quantity relative to other chemotaxis proteins. A Western blot or other similar method of quantifying protein production would be helpful in determining similarity to wild type protein levels.

In the case of the two deletions strains with suspected polar mutations, the regions of interest could be sequenced and aligned with their respective genomic database entries. This, along with development of native gene plasmids, would help clear up whether these assays accurately represent the ability of *cheY* and *fliM*.

Chapter 4: Future Directions

Since developing these fluorescent fusion strains, I have considered a number of experimental applications for them. Below I propose two primary research objectives to further characterize the chemotaxis system of *B. subtilis*. The first deals with the clustering patterns of coupling proteins (CheW and CheV) and the second discusses the development of a proposed system for monitoring response and adaptation to chemostimulation.

Objective 1: Identify the Clustering Behavior of *B. subtilis* Coupling Proteins Throughout the Cycle of Stimulation and Adaptation.

This series of experiments would provide fluorescent live-cell images of CheW and CheV localizations within *B. subtilis*. The exact functions of these two coupling proteins are not well understood within the context of the chemotaxis signaling cluster. Some bacterial species, such as *E. coli*, have only a single coupling protein, while others, such as *H. pylori*, have as many as three CheV analogs (1, 19).

Unlike the well-studied *E. coli* model, which has been shown to have highly static signal clusters, *B. subtilis* signal clusters appear to be dynamic, shifting along the poles and long sides of the cell in response to chemostimuli (44). In order to develop a complete model of cluster organization, this dynamic clustering behavior must be examined. The coupling proteins CheW and CheV, because of their crucial role in chemotaxis, make excellent targets for studying cluster reorganization.

Based on a previous immunofluorescence study by Wu *et al.* (44), I would expect to see CheW and CheV generally occupying separate regions of the subcellular architecture and shift positions during stimulation and adaptation. The Wu *et al.* study leaves several questions unanswered, however. What happens to clusters in-between stimulation and adaptation periods? How rapidly do the clusters reorganize? Can these shifts be tied to any other chemotaxis protein reorganizations?

As stated earlier, a live-cell protein localization model would be more flexible than the immunofluorescence-based experiments seen previously. While cells remain immobilized, they can be continuously imaged over the course of one or more attractant stimulation events. A live-cell model would also eliminate the need for membrane permeation prior to imaging.

I propose that it would be useful to create a *B. subtilis* strain which lacks both wild type CheW and CheV, expressing instead CheW-EYFP and CheV-ECFP. This strain would allow me to identify the locations of each protein and then I could monitor, in real time, how protein localization changes as the cells respond to changing attractant conditions. Subsequent experiments could then be conducted to place these proteins in context with other components of chemotaxis signal clusters. This live-cell fluorescence fusion assay would support previous findings (44), while adding to the overall understanding of cluster formation and migration in response to stimuli.

Strain Design and Qualification

In order to develop the above strain, I would need to establish that the fusions localize and function in a way that is similar to their wild type counterparts. The

following are diagnostic steps that would test my strain for protein production levels and chemotaxis function.

Based on the findings in Chapter 3, I would choose the CheW-EYFP and CheV-ECFP molecules shown to be most successful in complementing native protein phenotype. Genes encoding these fusions would then be inserted into the chromosome of a $\Delta cheW\Delta cheV$ deletion mutant. Together, these two fusions would be expected to at least partially complement wild type swimming function.

This insertion could be handled in a number of different ways, each with its own merits. I would likely use the Xer-cise method (4) detailed in Chapter 3 or a similar markerless insertion method. The fusions genes could then be inserted into their native positions in the chromosome, controlled by the native promoter for the Che operon. A Western blot probing with CheW- or CheV-specific antibodies could then be performed to compare protein production levels in the mutants to the wild type strain.

In the event that protein productions levels differ from native levels too dramatically, are insufficient to complement chemotaxis function, or are not great enough to form a visible fluorescence signal under a microscope, an alternative technique could be employed. Here, each fusion could be inserted into an ectopic location on the chromosome, under the control of an inducible promoter. This would prevent the fusions from interfering with native operon function and make protein production levels much more flexible (17).

One reason the HAP chemotaxis system is a good model for studying signal transduction is the numerous ways to measure the chemotaxis phenotype. These latest four strains would be compared to wild type both by a motility agar test (diameter of

swimming, as in Chapter 3) and by tracking the tumble/run frequency of swimming cells in a wet mount (using LabTrack software by BioRas). If further analysis is needed, a tethered cell assay could provide data on both rotational speed and directional switching frequency. Likewise, a chemotaxis capillary assay could provide further quantitative evidence of chemotaxis effectiveness (ability to traverse an attractant gradient) to accompany the motility agar data (15). This series of experiments would identify which strains can be induced to behave similarly to wild type.

Next, I would image this final fluorescent strain using a confocal laser scanning microscope, or CLSM. The cells would be grown to mid-log, stained with a general membrane stain (red FM 4-64), tethered (using either poly-L-lysine or Rain-X hydrophobic coating) to the surface of a glass-bottomed microwell dish and imaged prior to chemostimulation. Since the cells would have been tested in motility agar at 30°C, I would use an incubated stage apparatus to observe them at this same temperature. The cells would then be exposed to an attractant (asparagine) and imaged during stimulation and subsequent adaptation.

In each captured image, cells would have to show evidence of both red membrane dye signal and fluorescent protein signal to be considered “candidate cells.” Others would be excluded from

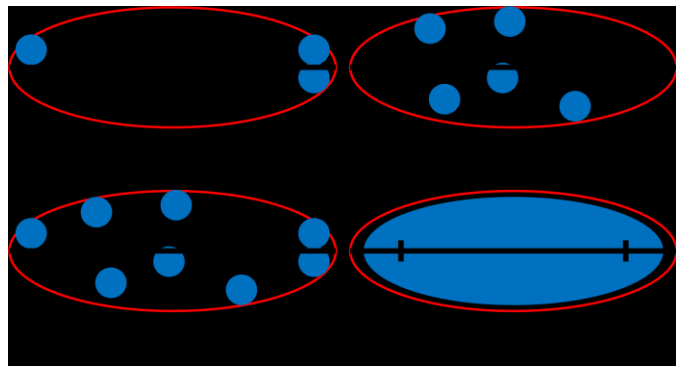


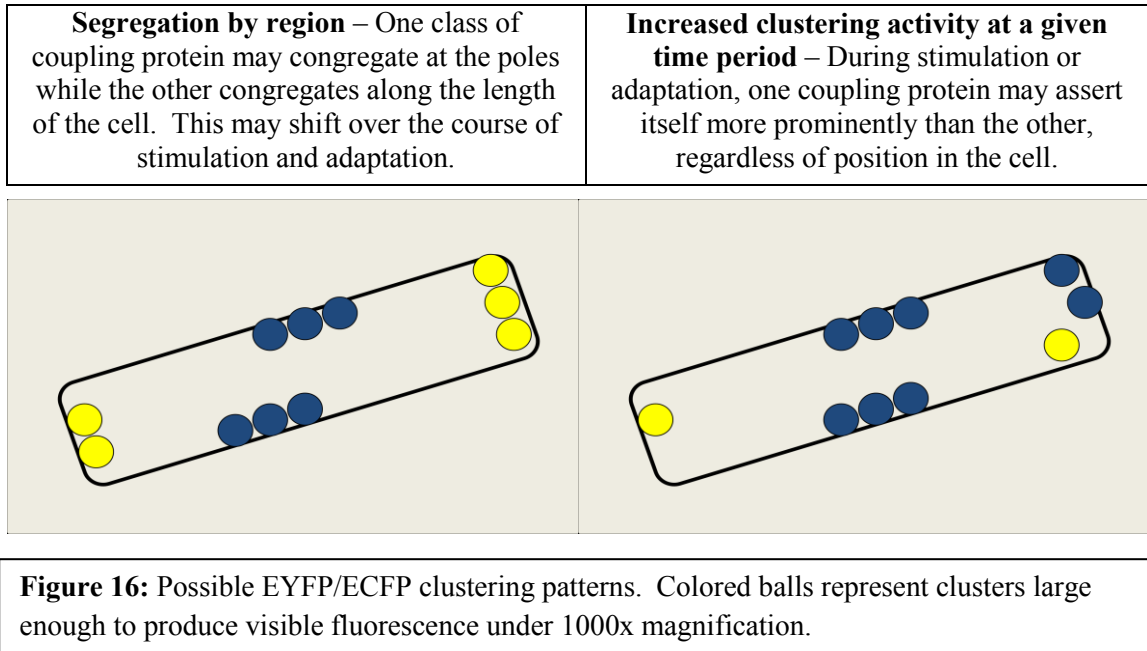
Figure 15: Cell Phenotype Metric. All cells must first have both a dye and a fluorophore signal. Each cell will be divided into 6ths. Dots in the outer 6ths are called “polar.” Dots in the interior 6ths are called “lateral.” Cells containing both types are considered “both.” Nonspecifically bright cells are called “diffuse.”

recording. Next, I would apply a phenotype metric (Figure 15) to these cells to determine their clustering phenotype. In this metric, a longitudinal line is drawn from pole to pole, determined by the tips of the red membrane. Each fluorescent fusion's signal is then measured separately. EYFP or ECFP emissions (measured from the center of fluorescence) within the first or last sixth of a cell's length are considered "polar." Specific fluorescence anywhere between these two regions is considered "lateral." Cells exhibiting points of fluorescence clearly in both regions are considered "both." Cells that completely fill their volume with fluorescence (non-specifically) are considered "diffuse." 100 candidate cells would be applied to the metric for any given strain in an experiment.

Next, I would look for changes in fluorescence localization as candidate cells respond to stimulation. The response patterns might be readily apparent from cell images. If they turn out to be more subtle, a comparison of histograms (showing coloration differences throughout the cell) at logical timepoints might prove useful. These changes in fluorescence could also be compared to the previously recorded tumble/run frequency mentioned above. I would expect to see a correlation between rotational switching and cluster rearrangement, as they are thought to be two ends of the same circuit.

During image analysis I would expect to see two distinct features. First, I would expect CheW and CheV to congregate in different regions of the cell, as seen previously (44). Second, I would expect each protein to respond to stimulation by either changing location or becoming more or less bright/concentrated (see Figure 16). Patterns that

emerge from this analysis would be used to craft future experiments to elucidate how the two proteins differ in function.



Objective 2: Develop a FRET Assay to Monitor *B. subtilis* Chemostimulus Response and Adaptation.

B. subtilis chemotaxis signaling adaptation diverges significantly from the *E. coli* paradigm. This series of experiments would monitor the interactions between the response regulator (CheY) and the flagellar switch protein (FliM) before, during, and after stimulation by an attractant. Once a model has been established for tracking these interactions, further studies would be conducted to determine if and how these interactions change when each of the adaptation mechanisms is disrupted.

In Regard to Results from Chapter 3

The motility plate assays in Chapter 3 demonstrate that the CheY and FliM genetic constructs (shown in Figures 11 and 12) are not yet ready to be implemented in the following experiment. However, if the issue with both sets of strains can be traced to the method or implementation of native gene deletion, then the fluorescent fusions may yet be useful once a deletion strain has been developed that can be successfully rescued. Of all the genes described in this thesis, CheY and FliM are the most recent to be focused upon and have accordingly received the least time and attention. Indeed, I believe more troubleshooting (including comparing the function of the fusion proteins to the native proteins) needs to be done before either the general research strategy or the experiment below is discarded.

Constructing a FRET Assay to Monitor the Interaction Between CheY and FliM *in vivo*

In bacterial flagellar chemotaxis, the crucial step of signal transduction is the interaction between the response regulator and the flagellar switch protein, in this case, CheY(-P) and FliM. By measuring how often these proteins interact, it is possible to quantify the amount of signal reaching the flagellar motor complex.

One method of measuring protein-protein interactions is Förster Resonance Energy Transfer (FRET). As described in Chapter 2, FRET assays take advantage of a measurable interaction between YFP and CFP molecules in close proximity. *E. coli* chemotaxis researchers have gained many insights from a *cheY-eyfp* and *cheZ-ecfp* (CheZ is a CheY-P phosphatase in *E. coli*) pair used to measure rates of response and adaptation to chemoattractants (18, 33). The example FRET graph (Figure 17) shows a static emission signal that is perturbed by an increase in asparagine (an attractant in *B. subtilis*) (39). This results in a dramatic increase in emission signal, referred to here as “stimulation” of the chemotaxis pathway. Eventually the emission signal returns to its previous state, an event referred to as “adaptation.”

I would create a *B. subtilis* strain expressing both EYFP-CheY and ECFP-FliM. FliM can only interact with CheY-P and represents the end of the chemotaxis circuit (32, 39). Each fusion would be inserted ectopically (under the control of independent promoters) into a $\Delta cheY\Delta fliM$ deletion mutant and tested for a restored swimming phenotype and normal production protein levels as described in Objective 1. Once my mutant strain had been set up, I would perform a FRET study.

The FRET measurement protocol I would use is based on work by Sourjik and Berg and was adapted by the Stewart lab (32, 39). The fluorescent emission of a suspension of the $\Delta cheY \Delta fliM \Omega P_{lac} eyfp-cheY P_{xyl} ecfp-fliM$ strain would be excited at $\sim 480\text{nm}$ and monitored in a spectrofluorometer (PTI QuantaMaster) until $\sim 535\text{nm}$ emissions plateau. Chemoattractants, such as asparagine, could then be added to the cuvette and the response would be recorded as a variation in emission signal.

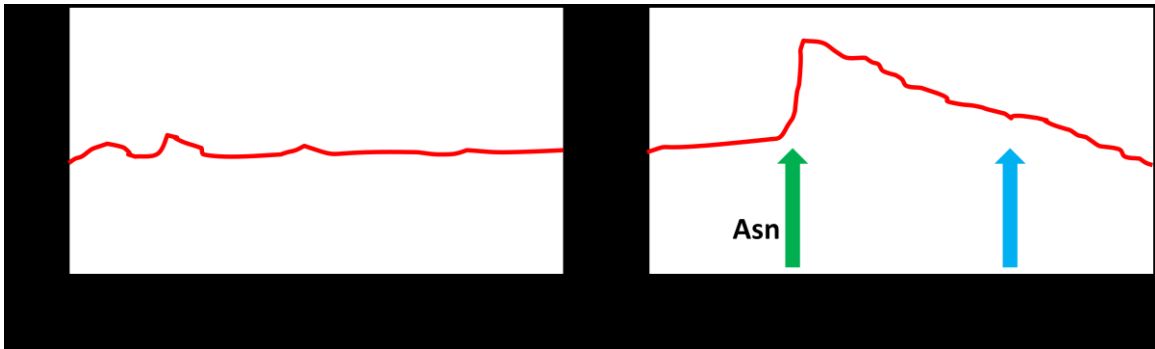


Figure 17: An example EYFP emission signal during a CheY-EYFP and FliM-ECFP FRET experiment in *B. subtilis*. (Left) A baseline EYFP emission signal: ECFP is being excited and some EYFP signal is being emitted at a somewhat constant rate. (Right) The green arrow indicates the addition of the attractant asparagine to the cuvette. This arrow also indicates the immediate excitation of the chemotaxis signal clusters, evident by an increase in EYFP signal output, the result of more FRET occurring. This spike immediately begins to level off until it reaches the blue arrow, where emission signals have returned to their baseline levels (or just below).

To show that the strain is indeed producing a FRET signal, there are several controls I could set up. First I would record the background level of fluorescent emission in the wild type *B. subtilis* strain. Then I would record emissions from strains with only one of the fluorescent fusions present (excited by the appropriate wavelengths) and adjust the recorded value by the average background fluorescence. In my double deletion, double fusion model strain, I would expect to see a reduction in previous ECFP emissions as EYFP absorbs energy that would otherwise be emitted by ECFP (25). This dip in

ECFP emissions would provide evidence to support any EYFP emissions that were inferred to be the result of FRET, as both the reduction in ECFP emissions and the increase in EYFP emissions should happen simultaneously.

Conversely, on the stage of a CLSM, I could record ECFP emissions in the model strain and then photobleach the EYFP molecules as described in Sourjik *et al.* (33). I would expect the ECFP emissions to increase after photobleaching, as the energy that was previously transferred by FRET remains among the ECFP emissions.

In order to provide evidence that the FRET signals are biologically relevant to the signal pathway in question, I would develop several control strains.

First, I would create a CheY mutant that could not be phosphorylated. The simplest way to accomplish this would be to change the key Asp54 residue to another amino acid such as Ala (this mutant would be fused to EYFP and inserted ectopically like its functional counterpart) as done previously in both *E. coli* (35) and *B. subtilis* (2). I would expect this to produce a highly tumbling mutant strain. It would also provide a negative control for the FRET experiments, showing that a loss in CheY-P binding function will also prevent the FRET reaction (as the phosphate is necessary for FliM binding).

Similarly, a constitutively active CheY mutant would be useful. It would logically result in a strain that “runs” constantly. I have been unable to find an example of such a mutant in the literature, but the dramatic change in phenotype should make screening for a running mutant possible. It would have very poor swimming/chemotaxis abilities in motility agar and would spin CCW on a tethered cell assay. More elaborate

solutions have been developed for creating constitutively active CheY mutants in *E. coli* (9), but it is unclear whether these strategies would transfer to *B. subtilis*.

Identifying the Contributions of Several Adaptation Mechanism in *B. subtilis*

Chemotaxis

Unlike *E. coli*, *B. subtilis* has at least three adaptation mechanisms that can modulate signal transduction before, during, and after attractant stimulation. Using the above FRET assay, I would make a quantitative assessment of the effect that each *B. subtilis* adaptation mechanism has on the system's response to an attractant.

Starting with the same strain ($\Delta cheY \Delta fliM \Omega P_{lac} eyfp-cheY P_{xyl} ecfp-fliM$), I would additionally delete either *cheC* and *cheD*, *cheB* and *cheR*, or *cheV*. To substitute for a *fliY* deletion strain, which has been shown not to form flagella, I would replace the wild type gene with a *fliY* allele that encodes a mutant FliY with no phosphatase activity (36). Each deletion strain would then be measured in the FRET spectrofluorometer assay and those measurements would be compared to the parental strain (containing all adaptation components).

I expect that the $\Delta cheC \Delta cheD$ and $\Delta cheB \Delta cheR$ mutants would both increase the amount of time required for CheY-P/FliM interactions to return to a pre-stimulatory level. Deletion of a functional *fliY* would probably increase the number of pre-stimulatory CheY-P/FliM interactions. It would also shift the task of dephosphorylating CheY-P to CheC alone.

It is unclear what effect a *cheV* deletion would have on the FRET emission level, but if the role of CheV is to maintain a stable pre-stimulatory level of CheY-P (by

accepting excess phosphates from CheA-P), then the strain might show an increased or fluctuating level of CheY-P/FliM interactions prior to stimulation. If CheV plays a role in adaptation after stimulation, it might instead resemble the delayed adaptation response proposed for $\Delta cheC\Delta cheD$ and $\Delta cheB\Delta cheR$.

One of the major findings that could emerge from this experiment is the relative importance of each adaptation mechanism. CheB and CheR might turn out to dramatically effect adaptation times, but CheC and CheD might have only a small impact. Alternatively, different mechanisms may prove more important at different points in the cell's journey up the attractant gradient. Small concentrations of attractant might utilize one system, but once attractant concentrations become too high, a different mechanism might perform more efficiently.

Summary

I am optimistic that the experiments described herein would provide new insights about the architecture of *B. subtilis* chemotaxis signaling. Both objectives would develop clear methods for investigating protein localization and protein interaction. Studies of *E. coli* have shown a relatively simple adaptation system that relies heavily on receptor methylation states. In *B. subtilis*, we see a much more complex adaptation system. Numerous steps in the stimulation pathway appear to be modulated by several distinct adaptation mechanisms. There are also two distinct coupling proteins (compared to the one in *E. coli*) that seem to behave independently of one another and may influence adaptation. These attributes are not only significant in their contrast with *E. coli*, but because many of the components are likely found in organisms studied regularly by medical researchers (1, 19). It is a further sign that our understanding of bacterial

diversity and complexity is still small when compared to the myriad signal transduction and regulation systems in the microbial tree of life.

Appendix A

Table 3: List of Primers Used in this Work

3a) Xer-cise primers for *cheA* deletion strain

Name	Restriction Site	Sequence (5' to 3')
XerALFup	BstEII	AAG <u>GTAACC</u> ACGGCTGTGTTACATAGCA
XerALFdn	MluI	GA <u>ACGCGT</u> CTGATTCATATCCATTTGAATCA
XerUpARF	NheI	AAGCTAGCGCACTGATTATTTAACCATTCCG
XerDnARF	Sall	TT <u>GTCGAC</u> ACACATCCGTATCTTTCTGAAC

*Restriction sites are underlined.

3b) Fluorescent fusion primers for *cheA*

Name	Restriction Site	Sequence (5' to 3')
JRbscheA-up2	BamHI	ACAT <u>GGATCC</u> ATGGATATGAATCAGTATTT
JRbscheA-dn2	N/A	<i>TCCGCCTCCGCCTCCAATAATCAGTGCATTACAAT</i>
JRbscheA-up1	N/A	<i>GGAGGCGGAGGCGGAATGGATATGAATCAGTATTT</i>
JRbscheA-dn1	XmaI	ACAT <u>CCCGGGT</u> TAAATAATCAGTGCATTAC

*Restriction sites are underlined. Glycine linker region is italicized.

3c) Xer-cise primers for *cheW* deletion strain

Name	Restriction Site	Sequence (5' to 3')
BsW5up	BstEII	AAT <u>GGTGACCT</u> CTATTCAGCATCCAGCTGC
BsW5dn	MluI	CA <u>ACGCGT</u> CTGCAGTCATGTGAGACACCT
BsW3up	NheI	AAGCTAGC <u>CCGATCAAGCTTAATCTTAAAG</u>
BsW3dn	Sall	CT <u>GTCGAC</u> ATGTCCAATGAGACTTCAGGA

*Restriction sites are underlined.

3d) Fluorescent fusion primers for *cheW*

Name	Restriction Site	Sequence (5' to 3')
CheWEYFPFusUpv3	BamHI	ACAT <u>GGATCC</u> ATGACTGCAGAAATTA AAAA CAGGCG
CheWEYFPFusDnv3	N/A	<i>TCCGCCTCCGCCTCCAGCTTGATCGGGCACAGC</i>
EYFPCheWFusUp	N/A	<i>GGAGGCGGAGGCGGAATGACTGCAGAAATTAAAAACAGG</i>
EYFPCheWFusDn	XmaI	ACAT <u>CCCGGGT</u> TAAAGCTTGATCGGGCACAG

*Restriction sites are underlined. Glycine linker region is italicized.

3e) Xer-cise primers for *cheV* deletion strain

Name	Restriction Site	Sequence (5' to 3')
BsV5up	BstEII	AAT <u>GGTGACCGACA</u> ACCAGCTGATTTGATTGT
BsV5dn	MluI	CA <u>ACGCGT</u> AACGACAATTCAATCCCTCG
BsV3up	NheI	AAGCTAGC <u>GAATAAATAAAAA</u> CAGCCGTTGC
BsV3dn	Sall	CT <u>GTCGAC</u> GAAACCGCCATGCA AAAA AC

*Restriction sites are underlined.

3f) Fluorescent fusion primers for *cheV*

Name	Restriction Site	Sequence (5' to 3')
CheVECFPUpv3	BamHI	ACAT <u>GGATCC</u> ATGTCGTTACAACAATACGAAATTTTATTGG
CheVECFPDnv3	N/A	<i>TCCGCCTCCGCCTCCTTCAATAACATACGTATCCACTTTTAAATC</i>
ECFPCheVUpv3	N/A	<i>GGAGGCGGAGGCGGAATGTCGTTACAACAATACGAAATTTTATTGG</i>
ECFPCheVDnv4	XmaI	ACAT <u>CCCGGG</u> TAAATAATCAGTGCATTAC

*Restriction sites are underlined. Glycine linker region is italicized.

3g) Xer-cise primers for *cheY* deletion strain

Name	Restriction Site	Sequence (5' to 3')
BsY-5up	BstEII	AAT <u>GGTGACCT</u> ATTGAACCGAAGCAACAGCAG
BsY-5dn	MluI	CA <u>ACGCGT</u> ATGTGCCATAATCTATCTCTCC
BsY-3up	NheI	AAG <u>CTAGCACAT</u> TAAAAATAAAGGGTGTACGACTG
BsY-3dn	SalI	CT <u>GTCGACG</u> TATGGATCTGTTCTGACCGAC

*Restriction sites are underlined.

3h) Fluorescent fusion primers for *cheY*

Name	Restriction Site	Sequence (5' to 3')
CheYECFPFusUp	BamHI	ACAT <u>GGATCC</u> ATGGCACATAGAATTTTAATTGTAG
CheYECFPFusDn	N/A	<i>TCCGCCTCCGCCTCCTTAATTTAATGTTTTGTTGATTGCTTC</i>
ECFPCheYFusUp	N/A	<i>GGAGGCGGAGGCGGAATGGCACATAGAATTTTAATTGTAG</i>
ECFPCheYFusDn	XmaI	ACAT <u>CCCGGG</u> TAAATTTAATGTTTTGTTGATTGCTTC

*Restriction sites are underlined. Glycine linker region is italicized.

3i) Xer-cise primers for *fliM* deletion strain

Name	Restriction Site	Sequence (5' to 3')
XerMLFupv2	BstEII	AAGGTAACCTAATTGGTGCTCTCGGGG
XerMLFdnv2	MluI	GA <u>ACGCGT</u> AACTTCTCCTGACATTTTCCTC
XerMRFupv2	NheI	AAGCTAGC CAAGATGGAGAATAATAGATTATCTCAAG
XerMRFdnv2	SalI	TT <u>GTCGACCG</u> CACTTAAATGGATTTCACC

*Restriction sites are underlined.

3j) Fluorescent fusion primers for *fliM*

Name	Restriction Site	Sequence (5' to 3')
FliMECFPFusUp2	AatII	ACAT <u>GACGTC</u> ATGTCAGGAGAAGTTCTCTCCCAA
FliMCFPFusDn	N/A	<i>TCCGCCTCCGCCTCCTTCTCCATCTTGTTACCTCTTAT</i>
CFPFliMFusUp	N/A	<i>GGAGGCGGAGGCGGAATGTCAGGAGAAGTTCTCTCCCAA</i>
CFPFliMFusDn	XmaI	ACAT <u>CCCGGG</u> TATTCTCCATCTTGTTACCTCT
ECFPAatIIup	AatII	ACAT <u>GACGTC</u> ATGGTGAGCAAGGGCGAGGA

*Restriction sites are underlined. Glycine linker region is italicized.

3k) Fluorescent fusion primers for *eyfp* and *ecfp*

Name	Restriction Site	Sequence (5' to 3')
JRey-up2	N/A	<i>GGAGGCGGAGGCGGAATGGTGAGCAAGGGCGAGGA</i>
JRey-dn2	XmaI	ACAT <u>CCCGGGT</u> TA <u>CTTGTACAGCTCGTCCA</u>
JRey-up1	BamHI	ACAT <u>GGATCC</u> ATGGTGAGCAAGGGCGAGGA
JRey-dn1	N/A	<i>TCCGCCTCCGCCTCCCTTGTACAGCTCGTCCATGC</i>

*Restriction sites are underlined. Glycine linker region is italicized.

3l) Primers used to created the difCAT region

Name	Sequence (5' to 3')
<u>my5bacDifCAT</u>	AATGGTGACCAACGCGTACTTCCTAGAATATATATTATGTAAACTTATTCTT CAACTAAAGCACCCATTAGTTCAACAAACGAAA
<u>my3bacDifCAT</u>	TTGGTCGACTGCTAGCAGTTTACATAATATATATTCTAGGAAGTGGATCGGC GAGGCTAGTTACCCTTAAGTTATTGGTATGAC

Appendix B

Contributors to this Work

Stewart Laboratory, University of Maryland, College Park

Dr. Richard C. Stewart

- Development of the difCAT TOPO plasmid construct (pCR4::difCAT).
- Development of Xer-cise deletion plasmids for *cheW* and *cheV*
 - pCR4::difCAT*cheW*
 - pCR4::difCAT*cheV*

Petya Lozanova

- Development of an Xer-cise deletion plasmid for *cheY*
 - pCR4::difCAT*cheY*

CBMG Imaging Core Facility, University of Maryland, College Park

Amy Beaven

- Provided training and technical support during collection of confocal images.

Ordal Laboratory, University of Illinois at Urbana-Champaign

Dr. George Ordal

- Development of *B. subtilis* strain OI1085 (Che⁺ *ilvC1 leu-1 trpF7 hisH2 metC1*)
 - Ullah, A.J.H. and Ordal, G.W. (1981) In vivo and in vitro chemotactic methylation in *Bacillus subtilis*. J. Bacteriol. 145: 958-965.

Bibliography

1. **Alexander, R. P., A. C. Lowenthal, R. M. Harshey, and K. M. Ottemann.** 2010. CheV: CheW-like coupling proteins at the core of the chemotaxis signaling network. *Trends in microbiology*. Elsevier Ltd **18**:494–503.
2. **Bischoff, D. S., R. B. Bourret, M. L. Kirsch, and G. W. Ordal.** 1993. Purification and characterization of *Bacillus subtilis* CheY. *Biochemistry* **32**:9256–61.
3. **Bischoff, D. S., and G. W. Ordal.** 1992. *Bacillus subtilis* chemotaxis: a deviation from the *Escherichia coli* paradigm. *Molecular microbiology* **6**:23–8.
4. **Bloor, A. E. A., and R. M. Cranenburgh.** 2006. An efficient method of selectable marker gene excision by Xer recombination for gene replacement in bacterial chromosomes. *Applied and Environmental Microbiology*. American Society for Microbiology **72**:2520–2525.
5. **Cabeen, M. T., and C. Jacobs-Wagner.** 2010. The bacterial cytoskeleton. *Annual review of genetics* **44**:365–92.
6. **Cannistraro, V. J., G. D. Glekas, C. V. Rao, and G. W. Ordal.** 2011. Cellular stoichiometry of the chemotaxis proteins in *Bacillus subtilis*. *Journal of bacteriology* **193**:3220–7.
7. **Carballido-López, R., and J. Errington.** 2003. A dynamic bacterial cytoskeleton. *Trends in Cell Biology* **13**:577–583.
8. **DeRosier, D. J.** 1998. The turn of the screw: the bacterial flagellar motor. *Cell* **93**:17–20.
9. **Dyer, C. M., M. L. Quillin, A. Campos, J. Lu, M. M. McEvoy, A. C. Hausrath, E. M. Westbrook, P. Matsumura, B. W. Matthews, and F. W. Dahlquist.** 2004. Structure of the constitutively active double mutant CheYD13K Y106W alone and in complex with a FliM peptide. *Journal of molecular biology* **342**:1325–35.
10. **Fredrick, K. L., and J. D. Helmann.** 1994. Dual chemotaxis signaling pathways in *Bacillus subtilis*: a sigma D-dependent gene encodes a novel protein with both CheW and CheY homologous domains. *Journal of bacteriology* **176**:2727–35.
11. **Fuhrer, D. K., and G. W. Ordal.** 1991. *Bacillus subtilis* CheN, a homolog of CheA, the central regulator of chemotaxis in *Escherichia coli*. *Journal of bacteriology* **173**:7443–8.

12. **Garrity, L. F., and G. W. Ordal.** 1995. Chemotaxis in *Bacillus subtilis*: how bacteria monitor environmental signals. *Pharmacology & therapeutics* **68**:87–104.
13. **Garvis, S., A. Munder, G. Ball, S. de Bentzmann, L. Wiehlmann, J. J. Ewbank, B. Tümmeler, and A. Filloux.** 2009. *Caenorhabditis elegans* semi-automated liquid screen reveals a specialized role for the chemotaxis gene *cheB2* in *Pseudomonas aeruginosa* virulence. *PLoS pathogens* **5**:e1000540.
14. **Gotoh, Y., Y. Eguchi, T. Watanabe, S. Okamoto, A. Doi, and R. Utsumi.** 2010. Two-component signal transduction as potential drug targets in pathogenic bacteria. *Current opinion in microbiology*. Elsevier Ltd **13**:232–9.
15. **Han, G., and J. J. Cooney.** 1993. A modified capillary assay for chemotaxis. *Journal of Industrial Microbiology* **12**:396–398.
16. **Karatan, E., M. M. Saulmon, M. W. Bunn, and G. W. Ordal.** 2001. Phosphorylation of the response regulator CheV is required for adaptation to attractants during *Bacillus subtilis* chemotaxis. *The Journal of biological chemistry* **276**:43618–26.
17. **Kearns, D. B., and R. Losick.** 2005. Cell population heterogeneity during growth of *Bacillus subtilis*. *Genes & development* **19**:3083–94.
18. **Kentner, D., and V. Sourjik.** 2009. Dynamic map of protein interactions in the *Escherichia coli* chemotaxis pathway. *Molecular Systems Biology* **5**.
19. **Lertsethtakarn, P., K. M. Ottemann, and D. R. Hendrixson.** 2011. Motility and chemotaxis in *Campylobacter* and *Helicobacter*. *Annual review of microbiology* **65**:389–410.
20. **Mikkelsen, H., M. Sivaneson, and A. Filloux.** 2011. Key two-component regulatory systems that control biofilm formation in *Pseudomonas aeruginosa*. *Environmental microbiology* **13**:1666–81.
21. **Moszer, I.** 1998. The complete genome of *Bacillus subtilis*: from sequence annotation to data management and analysis. *FEBS Letters* **430**:28–36.
22. **Moszer, I., P. Glaser, and A. Danchin.** 1995. SubtiList: a relational database for the *Bacillus subtilis* genome. *Microbiology* **141 (Pt 2)**:261–268.
23. **Muff, T. J., and G. W. Ordal.** 2007. The CheC phosphatase regulates chemotactic adaptation through CheD. *The Journal of biological chemistry* **282**:34120–8.

24. **Nguyen, H. D., Q. A. Nguyen, R. C. Ferreira, L. C. S. Ferreira, L. T. Tran, and W. Schumann.** 2005. Construction of plasmid-based expression vectors for *Bacillus subtilis* exhibiting full structural stability. *Plasmid* **54**:241–8.
25. **Overton, M. C., and K. J. Blumer.** 2002. Use of fluorescence resonance energy transfer to analyze oligomerization of G-protein-coupled receptors expressed in yeast. *Methods (San Diego, Calif.)* **27**:324–32.
26. **Porter, S. L., G. H. Wadhams, and J. P. Armitage.** 2011. Signal processing in complex chemotaxis pathways. *Nature reviews. Microbiology.* Nature Publishing Group **9**:153–65.
27. **Rosario, M. M., K. L. Fredrick, G. W. Ordal, and J. D. Helmann.** 1994. Chemotaxis in *Bacillus subtilis* requires either of two functionally redundant CheW homologs. *Journal Of Bacteriology* **176**:2736–2739.
28. **Rudner, D. Z., and R. Losick.** 2010. Protein subcellular localization in bacteria. *Cold Spring Harbor perspectives in biology* **2**:a000307.
29. **Schulmeister, S., M. Ruttorf, S. Thiem, D. Kentner, D. Lebiecz, and V. Sourjik.** 2008. Protein exchange dynamics at chemoreceptor clusters in *Escherichia coli*. *Proceedings of the National Academy of Sciences of the United States of America* **105**:6403–8.
30. **Selvin, P. R.** 2000. The renaissance of fluorescence resonance energy transfer. *Nature structural biology* **7**:730–4.
31. **Sourjik, V., and H. C. Berg.** 2000. Localization of components of the chemotaxis machinery of *Escherichia coli* using fluorescent protein fusions. *Molecular microbiology* **37**:740–51.
32. **Sourjik, V., and H. C. Berg.** 2002. Receptor sensitivity in bacterial chemotaxis. *Proceedings of the National Academy of Sciences of the United States of America* **99**:123–7.
33. **Sourjik, V., A. Vaknin, T. S. Shimizu, and H. C. Berg.** 2007. In vivo measurement by FRET of pathway activity in bacterial chemotaxis. *Methods in enzymology* **423**:365–91.
34. **Stock, J. B., a J. Ninfa, and a M. Stock.** 1989. Protein phosphorylation and regulation of adaptive responses in bacteria. *Microbiological reviews.*
35. **Szurmant, H., M. W. Bunn, V. J. Cannistraro, and G. W. Ordal.** 2003. *Bacillus subtilis* hydrolyzes CheY-P at the location of its action, the flagellar switch. *The Journal of biological chemistry* **278**:48611–6.

36. **Szurmant, H., T. J. Muff, and G. W. Ordal.** 2004. Bacillus subtilis CheC and FliY are members of a novel class of CheY-P-hydrolyzing proteins in the chemotactic signal transduction cascade. *The Journal of biological chemistry* **279**:21787–92.
37. **Szurmant, H., and G. W. Ordal.** 2004. Diversity in Chemotaxis Mechanisms among the Bacteria and Archaea. *Microbiology and Molecular Biology Reviews. American Society for Microbiology* **68**:301–319.
38. **Terashima, H., S. Kojima, and M. Homma.** 2008. Flagellar motility in bacteria structure and function of flagellar motor. *International review of cell and molecular biology. Elsevier Inc.* **270**:39–85.
39. **Thakor, H., S. Nicholas, I. M. Porter, N. Hand, and R. C. Stewart.** 2011. Identification of an anchor residue for CheA-CheY interactions in the chemotaxis system of Escherichia coli. *Journal of bacteriology* **193**:3894–903.
40. **Vaknin, A., and H. C. Berg.** 2004. Single-cell FRET imaging of phosphatase activity in the Escherichia coli chemotaxis system. *Proceedings of the National Academy of Sciences of the United States of America* **101**:17072–7.
41. **Wadhams, G. H., and J. P. Armitage.** 2004. Making sense of it all: bacterial chemotaxis. *Nature reviews. Molecular cell biology* **5**:1024–37.
42. **Werhane, H., P. Lopez, M. Mendel, M. Zimmer, G. W. Ordal, and L. M. Márquez-Magaña.** 2004. The last gene of the fla/che operon in Bacillus subtilis, ylxL, is required for maximal sigmaD function. *Journal Of Bacteriology. American Society for Microbiology* **186**:4025–4029.
43. **Williams, S. M., Y.-T. Chen, T. M. Andermann, J. E. Carter, D. J. McGee, and K. M. Ottemann.** 2007. Helicobacter pylori Chemotaxis Modulates Inflammation and Bacterium-Gastric Epithelium Interactions in Infected Mice. *Infection and Immunity* **75**:3747–3757.
44. **Wu, K., H. E. Walukiewicz, G. D. Glekas, G. W. Ordal, and C. V. Rao.** 2011. Attractant binding induces distinct structural changes to the polar and lateral signaling clusters in Bacillus subtilis chemotaxis. *The Journal of biological chemistry* **286**:2587–95.